A Geophysical Evaluation of Avaldsnes

prepared for: Dagfinn Skre
Department of Archaeology, Conservation, and History
University of Oslo
Arkeologiseksjonen
Postboks 1008 Blindern
0371 Oslo, Norway

by: Tatiana Smekalova
Moesgård Museum
DK 8270 Højbjerg
Denmark

and

Bruce Bevan
Geosight
356 Waddy Drive
Weems, Virginia 22576, USA

date: 2 December 2009

Introduction

A geophysical test was done at Avaldsnes in order to estimate which geophysical techniques might be most suitable for the exploration of a larger area at this historical site. This test revealed that a magnetic survey may be particularly valuable. Several broad features were revealed in the field southwest of the church; these features are at a depth of 0.5 - 1 m underground and some of them might be hearths. In the test area that was northeast of the church, a large difference was found on either side of a stone wall. On the eastern side of the wall, features with a high magnetic contrast were found to extend as lines in a north-south direction and bedrock appears to be deeper than 1.5 m; on the western side of the wall, few magnetic features were located, and bedrock could be very shallow in some parts of this area. A summary of the findings of these surveys are plotted in Figure 5 (southwestern area) and Figure 29 (northeastern area).

While a resistivity survey may provide a good estimate of the thickness of soil over bedrock, it does not otherwise appear to be particularly suitable here. The electrical conductivity of the soil is too low for good measurements with a conductivity meter. When that conductivity meter is switched to its susceptibility mode, better measurements are possible, but these are still inferior to those of a magnetometer.

The figures are at the end of this report; blue text indicates hyperlinks, and these are primarily to those figures. The captions for the figures are detailed and provide an extended summary of this work.

This final report supercedes the preliminary report that was dated 14 June 2009; that earlier report can now be discarded.

Acknowledgments

Our thanks go to Dagfinn Skre for interrupting his work at the University of Oslo in

order to visit the site and explain to us his requirements for a future geophysical survey. Dagfinn arranged for lodging near the site and he also speeded the magnetic susceptibility survey with his assistance during that work.

Marit Synnøve Vea is the director of the Nordvegen Historic Center in Avaldsnes; this center explains the importance of this archaeological site to visitors. She was a constant help to us during out test. She supplied us with background materials and photographs of the site, and she also gave us many photographs of the geophysical survey as it was being done. We also appreciate the images that she supplied from the earlier radar survey in the southwestern field; this allowed a comparison with this geophysical test.

The Site

The historic site of Avaldsnes is found on the eastern side of the island of Karmøy; see Figure 1 . The first government for a united Norway was located at Avaldsnes; this was the residence of King Harald Fairhair in the 9th century.

The site is on a bluff that overlooks a 300-m wide channel that separates the island from the mainland; the elevation of the area of survey is about 25 m above sea level. Figure 2 shows the topography of the island, while Figure 3 includes several aerial views of the site and island.

Bedrock in the region is metamorphic; in an aeromagnetic map (Magnetic anomaly map of the world, http://ccgm.free.fr), the region is moderately magnetic. There is a now-inactive copper mine on the west coast of the island. Bedrock is exposed at less that one per cent of the land surface; in other parts of the site, the depth to bedrock is possibly less than 2 m. The soil contains a high fraction of sand; this is revealed by the soil that is seen on stakes that have been removed from the ground.

The ground is covered by grass; this has been mown in some areas. Otherwise, the grass and weeds were either tall (about 0.6 m), or at a medium height where the vegetation has been browsed by sheep. There are few trees or bushes in the area of potential survey.

Several buildings are standing in the historical area, and these are apparent in Figure 3. The tallest building is St. Olav's Church; this medieval church is constructed of stone and it is located on the highest point in the vicinity.

The area is rural, although it is near a more industrial region. Two ships were anchored in a harbor about 250 m to the north; these ships were idle although it is possible that work on rust removal and painting was being done, for the sound of a grinder was heard there. It appears that a metal-reclaiming industry is about 2 km to the north; heavy electromagnets may be there for lifting ferrous metals. There appears to be little in the way of heavy industry on the mainland directly to the east. A low frequency radio antenna has its wires arching across the channel between the island and the mainland; this group of antennas is a few kilometers to the south; no other transmitting antennas were visible nearby. Electric wires and pipes for the historic church, the Nordvegen

Historic Center, and the other buildings are underground, and their exact location is not known. No high voltage power lines or electrified railroads are in the vicinity. The town of Avaldsnes is about1 km to the west of the historic area. Almost no metallic trash was found in the areas of this survey.

The historic area, along with the modern cemetery next to the church, has frequent visitors. Perhaps fifty cars and a few buses visit every day; these vehicles park on the southern side of the church. Except for these visitors, there are no heavily-traveled roads in the area.

Some broad-area excavations were done at this site in prior centuries. In modern times, a few trenches have been dug across settlement areas. All of these excavations have been backfilled. Excavation reports were not available for these studies.

For the immediate future, the goal of excavation (and geophysics) is the study of early settlements through their houses. There are four major characteristics of the remains of these houses:

1: Post holes – These may be 25 - 35 cm wide and 30 cm deep. Stones may have been used to wedge the posts in the holes.

2: Hearths – A burned layer of clay may be found at these locations, and this clay circle or oval may be surrounded by stones. The hearths could be in the range of 1 - 4 m wide.

3: Cooking pits – These contain stones whose directions of magnetization may all be the same. A mixture of wood and stone was placed in a pit and burned; as the burning continued, the stones settled to the bottom of the pit. These hot stones later cooked the food that was being prepared. These now-filled pits may be 1 - 3 m in diameter.

4: Trench – This shallow and oval trench may outline the outer part of a house. This feature is expected to be so shallow that is it less likely to be detected than the features above. This is unfortunate, since the geometric shape of this feature is probably a certain guide to its identification.

Several years ago, a geophysical survey of the parking lot was done by Kjell Persson and a few others (from Sweden); a ground-penetrating radar and a Geonics EM38 were applied to that work and the report on this survey is available at the site. About a month before this geophysical test, a ground-penetrating radar survey was done in a field (called Hovedområde 1) southwest of the church by a person or group from Austria; time slices of the radar data from that survey were available at the time of this test.

The geophysical test was done in two separate areas; these are illustrated in Figure 3 and described further below. The geophysical grids were set up with an optical right-angle sight and several tape measures. Dagfinn assisted with setting up the grid northeast of the church.

southwest of the church - the Hovedområde 1 area

This test area is located about 80 m southwest of the church; Figure 4 is a ground-

level photograph of this area. The grass here had not been cut or grazed this year, and it was about 0.6 m tall; there are few or no weeds with the grass. The land surface dips down toward the south, and the relief in the area of survey is about 4 m. A ridge of soil extends to the south from the north edge of the grid, near its midpoint. There are no trees or bushes in the area. A shallow cliff rises just outside the western side of the area of survey and reveals bedrock at the surface.

A geophysical grid was set up at this location and it had dimensions of 80 m east-west and 50 m north-south; this duplicated the size of the grid that was applied to the earlier radar survey. During the setup of the grid, five short tree branches (0.1 - 0.3 m long) were found hidden and upright in the grass; the spacing between four of these revealed them to be corners of the grid for the radar survey; therefore, this geophysical test applied those corners and the two surveys may be compared easily and accurately. For this test, the southwestern corner of the 50 by 80 m rectangle was called reference point E100 N100. The five tree branches were left in place after the end of this test, and no further markers were placed to locate the grid. Magnetic north is about 6° west of grid north here. Maps and aerial photographs indicate that the near corner of the church is located at about E221 N207 in the coordinate system that was applied in this area.

Three sides of the grid (west, north, and east) are bordered (at a distance of 2 m or more) by a mesh fence of iron wire that is about 1.2 m high. Access to the area is over the fence at the northeastern corner of the area. The east side of the grid is 3 - 4 m from the edge of the main road to the church and visitors' center.

Two archaeological excavations have recently been done in this area. A pair of trenches, each about 3 m wide, 45 m long, and aligned about north-south (in this geophysical grid), were dug across most of the area of this test. In the coordinates of this test, the midlines of these trenches were located at about E124 (N92 to N135) and E169 (N91 to N142). The eastern trench found many more archaeological features of importance than the western trench; except for this, the findings of those excavations are not available for this geophysical analysis. Those trenches were refilled, and they were invisible during this field work. While there may be some subsidence of the soil that fills the trenches or perhaps shallow piles of excavated soil are nearby, these were not visible because of the tall grass.

northeast of the church - the Flag Hill area

This test area is about 50 m northeast of the church; part of the area is shown in the photograph of Figure 26. There was once a tall burial mound (about 45 m in diameter) in this area; it was removed at some past time and the soil was spread over the cemetery of the churchyard; this allowed burials where bedrock was shallow. It is possible that one edge of this former mound is revealed by a ring of soil (about 0.7 m tall) on the east side of that former mound; this is illustrated in Figure 28 and by the shadows in Figure 3. In this area, the goal of the geophysical test was an estimation of which geophysical instruments could be most suitable for detecting additional burials that might have been

placed before the mound was constructed.

A reference grid that was a square, and 30 m on a side, was set up in this area. The reference point E100 N100 for this grid was placed at the corner of a historic grave; see Figure 6. The stone wall (1 m wide and 1 m tall) that is shown there, along with the location of this grave, will allow this grid to be relocated at any time in the future. All stakes were removed after this geophysical test. Magnetic north is about 4° west of grid north here.

The relief in the area of this grid is about 2 m; however, there are steep slopes just outside the west, north, and east sides of the grid. Within the grid, no bedrock is visible; the fraction of sand in the soil here appears to be lower than what was found in the test of the field that is southwest of the church.

There is an electric fence on the east side of the stone wall. This has wooden posts and aluminum wire; it was not activated and no sheep were in the vicinity during this geophysical work. Several graves from the modern period are found in the southwest quadrant of the area of test; no geophysical work was done in that area.

The Geophysical Surveys

Three geophysical instruments were applied to this test; sketches are included in Figure 34.

magnetometer

Special emphasis was put on a magnetic survey, since a magnetometer is excellent for locating important features that are expected in the southwestern area of this test: Hearths and cooking pits. Refilled earthworks, such as post holes and trenches, may also be detectable because the soil that now fills these features has been altered from its original stratigraphy; as an example, magnetic topsoil may have been replaced by less magnetic subsoil.

With a magnetic survey, the magnitude of the Earth's magnetic field is measured; this is different from a magnetic compass, which measures the direction of the Earth's field. Underground objects that are magnetic can warp the Earth's field from its naturally simple patterns into complex patterns called anomalies; Figure 8 shows examples. A magnetometer, like that illustrated in Figure 27, can measure the magnetic field to an accuracy of better than one part per million. This high sensitivity allows weakly-magnetic objects to be detected to a depth of several meters underground.

A pair of identical magnetometers were used for this survey; these were Overhauser magnetometers, model GSM-19WG, that were manufactured by the Canadian firm of Gem Systems. One magnetometer was placed at a fixed point and measured temporal changes in the Earth's magnetic field at intervals of 15 s. The second magnetometer was carried along north-going traverses in the two geophysical grids; it was operated in its "walking mode", with readings at time intervals of 0.2 s. Recorded traverses were made only toward the north so that heading error would not affect the

survey. Markers were added to the digital recordings to indicate intervals of 1 m along each traverse. Because of a slightly irregular speed of walking, readings were made at somewhat irregular intervals, although their average spacing was about 0.2 m along each line. Lines of traverse were spaced by 0.5 m and parallel lines progressed toward the east. The height of the moving magnetic sensor was about 0.3 m above the soil's surface. The internal clocks of the two magnetometers were synchronized before each survey.

Lines of traverse were defined by a set of cords that were stretched along north-south lines across each area of survey; these cords had markers at intervals of 1 m and they were spaced at intervals of 2 m. It was easy to estimate distances of up to 1 m from these cords. The sequence of four traverses next to one cord could be as follows: Follow a path 1 m to the left of a cord, a second line 0.5 m to the left, the third line over the cord, and the fourth line 0.5 m to the right of the cord. The sequence would then be repeated at the next cord.

The tall grass in the southwestern field lowered the accuracy of placing these cords, and this caused minor difficulty with the magnetic maps. When a cord rests on top of the tall grass, the necessary tension on the cord can deflect the cord when the grass bends. The cords could not be placed at the base of the grass, for then the markers along the cords would be invisible. While it would be possible to elevate the end points of each cord above the grass, this would require tall and rigid stakes at the ends of each line, and each stake would have to be placed firmly in the soil (or be guyed) in order to support the tension of the cord.

susceptibility meter

An electromagnetic induction meter was applied to this test. This instrument was a model EM38, manufactured in Canada by Geonics. This geophysical instrument can measure both the electrical conductivity and magnetic susceptibility of the soil to a depth of about 1.5 m. In its conductivity mode, the instrument is excellent for detecting earthen contrasts, such as those between high conductivity materials (which may be clay or silt, or soil that is organic, saline, or moist) and low conductivity materials (which may be stone or sand, or perhaps dry soil). In its magnetic susceptibility mode, the EM38 is excellent for detecting fired earth and magnetic soils. This magnetic mode measures an effect that is somewhat different from that of a magnetometer: The EM38 detects the induced magnetization of a feature, and not its remanent (permanent) magnetization; a magnetometer measures both induced and remanent magnetization. The EM38 is better for detecting features with tapered or graded boundaries; a magnetometer detects abrupt boundaries the best. The magnetic susceptibility meter is less affected by nearby iron objects (such as a wire fence) than a magnetometer, but it is more strongly affected by electrical interference from power lines or lightning.

The Geonics EM38 is a small instrument, slightly more than 1 m in length. It has the appearance of a carpenter's level, with a few added dials and meters. Coils of wire are inside the instrument at its distant ends. An alternating magnetic field is transmitted

into the soil from one coil, while the other coil detects the magnetic field as it has been transmitted through, and altered by, the soil. Therefore, this instrument has similarity to an electrical transformer, and the mutual inductance between the two coils is measured. The alternations of the magnetic field in the receiving coil are slightly delayed from the field in the transmitting coil. This is a phase lag, and the received field can then be converted into two fields; one is in-phase with the transmitted field, and the other is out-of-phase by 90° from that transmitted field. While this sounds like dull electronics, it allows one to measure two very different parameters of the soil. The electrical conductivity is determined by the out-of-phase field while the magnetic susceptibility of the soil is determined by the in-phase field. It is valuable to be able to get two independent measurements from one instrument.

The EM38 was first tested in its conductivity mode. This was found to be inferior at this site. This was because the conductivity of the soil is very low, at about 1 - 2 mS/m (millisiemen per meter). The variability (or noisiness) of the values was about +/-1 mS/m and therefore reliable anomalies could not be detected. In its magnetic susceptibility mode, the instrument detected strong and clear anomalies from some features, and so this mode was applied to this test.

The data logger for this instrument had a recent failure and could not be repaired in time for this test; therefore, the measurements from the EM38 were simply written on paper. While this slowed the survey, it was still possible to explore a large enough area to show the capability of the instrument.

The EM38 was tested only in the southwestern area; Dagfinn assisted with this survey. The bar of the instrument was elevated to a height of 0.3 m. By lifting the EM38 from the ground's surface, it was easier to operate in the tall grass. While a greater height of 0.6 m would have simplified the analysis of the data, the anomalies were too weak at that greater height. At the height of 0.3 m, the instrument was still sensitive to its elevation; lowering the EM38 by a distance of 10 cm could cause the readings to about double. Therefore, the EM38 was held at a constant height with the aid of a rope over a shoulder that was tied to the middle of the instrument.

The magnetic dipoles of the EM38 were vertical and the length of the instrument's bar was oriented north-south. In order to simplify the processing of the data from the EM38, the instrument's zero value of susceptibility was set between each line of traverse; to do this, the instrument was held at a height of about 1.5 m in its horizontal dipole mode, and the I/P (in-phase) zeroing knob was adjusted to a value of about zero. This turned out to be a mistake, for the "zero" value was found to vary too much. It would have been better to have simply recorded the "nearly-zero" reading at each high reference point, and later to have adjusted for these changes. This is the procedure that has normally been applied with this instrument; this new procedure was simply an experiment that failed.

Measurements were made at intervals of 1 m along lines that were spaced by 1 m during the first test. This survey was done in the eastern side of the southwestern area. After that initial survey was done in an area of 50 by 16 m (Figure 17), a smaller area (10

by 10 m) was explored at a higher spatial resolution (with readings at 0.5 by 0.5 m). This resurvey is plotted in Figure 41. This detailed map shows linear striations that extend in the north-south direction; these defects were mostly eliminated by data processing (see Figure 23). This survey at a measurement spacing of 0.5 m was found to be distinctly superior to a measurement spacing of 1 m; the closer spacing allowed some anomalies to be revealed by enough measurements so that the shape of the features could be approximated.

At two times during the EM38 survey, negative spikes in the readings were noted; at first these readings were 6 - 10 mS/m too low, but within a second or so, the readings rose to a reasonable value. The cause of this temporal noise was not discovered. It could be sferic interference, for rain was noted to the south during the survey. It also could be interference from regional industries or power lines.

resistivity meter

The third tests were made with a resistivity meter, an AEMC model 4610 instrument from France. While low values of conductivity prevented the EM38 from getting good readings of that parameter, the inverse parameter of resistivity was readily measured with the resistivity meter. The features that can be detected by a resistivity meter are generally the same as those that are revealed with a conductivity meter.

The AEMC meter is a general-purpose instrument that can be applied to many different modes of measurement: Profiles, soundings, and pseudosections. It is an auto-ranging meter that measures resistance as high as 2000 ohm. Its current source is either 0.1, 1, or 10 mA, depending on the resistance; to get this current, the applied voltage rises as high as 42 V. The transmitted signal is a square wave that has a frequency of 128 Hz. It is powered by eight 1.5-V AA batteries, and these last for at least 1800 measurements; each reading is displayed on an LCD panel about 6 s after the starting button is pushed (the button can be held down to speed the survey).

The resistivity survey was done only in the area northeast of the church. The instrument was operated in the pole-pole configuration, and the spacing between the moving electrodes was 1 m. Readings were made at intervals of 1 m along five north-south lines; these measurements were recorded as resistance values in a notebook. Since the moving electrodes were set at integer meters along the traverses, the measurements were recorded at coordinates that were offset by 0.5 m (midway between the two moving electrodes). Figure 43 is a photograph of the survey, while Figure 33 shows the data that were measured.

The locations for the reference electrodes were selected depending on which side of stone wall was surveyed. For the three lines to the east of the stone wall, the current reference was located near E140 N115 and the voltage reference near E118 N130. For the two lines to the west of the stone wall, the reference electrodes were set downhill to the west and diagonal from the area of survey; their exact locations were not recorded.

The geophysical instruments that were applied to this test are the personal property

of Tatiana; their usage was donated to this project. Tatiana did all of the surveys with the magnetometer, Dagfinn and Bruce did the EM38 survey, and Bruce did the resistivity survey.

The tests in the southwestern area were made on 8 June 2009, and the work northeast of the church was done on 9 June. While there was a slight amount of rainfall on the first day, the second day was dry. Temperatures were seasonable and cool.

Data Processing and Analysis

This section is detailed and technical. The following section, Findings of the Geophysical Tests, describes the results of this analysis.

magnetometer

The first step in data processing was the addition of coordinates to each of the magnetic measurements. The digital files of the magnetic recordings have a sequence of data lines, and each line lists either a reading of the magnetic field and its time, or it is a traverse coordinate (marker or fiducial) than indicates that an additional 1-m distance has been walked. Typically, there were five measurements of the magnetic field between each coordinate marker. The software within the Gem magnetometer can interpolate coordinates for each of these five measurements; however, it does this with a slight inaccuracy: The first measurement after each marker is assigned the coordinate of that marker. If there were five readings between markers, their coordinates would be assigned as follows:

M M M
B B B B B B B B B B

where M indicates the coordinate of a marker, and B indicates the coordinate that is assigned to each of the readings of magnetic field. With this procedure, the measurements are shifted backwards (incorrectly) along each line by an average distance that is half of the spacing between readings. If the average measurement spacing was 0.2 m, there would be an average error (or consistent bias) of 0.1 m in the locations of the readings.

It would be more logical and more accurate to locate the readings as follows:

M M M
B B B B B B B B B B

With this procedure, there would be no consistent error in the locations of the measurements. While the average error with the procedure that is applied by Gem is only 0.1 m for this survey, it can be possible to estimate the central locations of underground objects to an accuracy of better than 0.1 m, and therefore an automatic or minimum error of 0.1 m is undesirable.

In order to avoid the error of 0.1 m in locations that would be provided by Gem's procedure, a separate computer program was written to add coordinates with the second, and more accurate, procedure. It is not known why Gem allowed a slight flaw into their

procedure; the added complexity of the improved procedure is very minor. Probably Gem felt that the error was insignificant.

The spatial readings were next corrected for temporal changes of the Earth's magnetic field using the GemLink program. This was done by subtracting the readings of the magnetic base station (Figure 36) from the spatial readings; a linear interpolation was made between the two nearest base station readings to the time of each of the spatial measurements.

The slight variability in the spacing of the magnetic measurements (from one marker to the next) was corrected by gridding; the spacing between interpolated field values was set to 0.25 m along north-south lines. A distance-weighted average of the two readings (along a north-south line) that were closest to each grid point was used to calculate the value for that grid point. Next, for convenience, the approximate value of the average or background field was subtracted from the gridded numbers. Then, the maps of total magnetic field were plotted.

These initial maps revealed a fault in the marker switch of the magnetometer. Within the last decade of using this magnetometer, the marker switch has been pushed about four million times (while walking a distance of about 8000 km). The electrical contact of the marker switch was erratic during this survey, and about 50 markers (of a total of over 8000) in the southwestern area were not recorded by the magnetometer. These missing markers could be identified in the initial magnetic maps by three methods. First, a count (made with a computer program) of the number of markers on each line of traverse showed that some lines were clearly missing one or more markers. Second, missing markers shifted a column of measurements improperly to the south and these shifts were revealed by anomalies (undulations of the contours lines) in the magnetic map that had a width of one measurement column. Third, if a span was found where suddenly there were twice the normal number of measurements between markers, a marker was certainly missing at the middle of that span.

This third method of locating missing markers seems to be the best, but it was not as successful as it could be for this data. This was because the speed of walking in this tall grass was more irregular than usual; short grass would not cause this problem. While there were typically about five readings made between markers, this walking speed was too variable to allow the marker spacing to reveal missing markers with certainty. In addition, there were usually more measurements made in the first meter of a traverse than in the following span; this was just an acceleration to walking speed. Furthermore, the speed of walking increased during the survey, from an average of 5.5 measurements per meter on the western side of the survey area to 4.5 measurements per meter at the end of the survey; this speedup is typical of geophysical surveys (it allows one to complete the survey of a required area in a day).

The first two procedures allowed the detection of those lines that had faults along them. The iron wire of the fence at the north side of the area of survey aided this analysis, for the fence causes a rather uniform gradient in the southwestern field. On those lines

where a marker was missing, the gradient from that fence was shifted to the south, and this was quite apparent in the magnetic map. In addition, anomalies farther to the south were also shifted and the source of the fault could be approximated by the location in the map where this shift was no longer apparent. The third procedure was next applied. A computer program provided a listing of the number of measurements between each marker; this listing was checked in the region where the initial examination suggested that a marker was missing. A marker was added to the middle of the span where the greatest number of measurements was found between a pair of markers in that vicinity.

The resulting magnetic map (Figure 10) shows that this correction worked well. Note that shifted anomalies are still apparent at about six locations at the extreme northern end of this map. While these reveal missing markers that have not been corrected, those missing markers were so close to the northern end of the map that they cause no difficulty for the analysis of the measurements. During the survey of the northeastern area, markers were found to be missing on only two lines; those errors have been corrected in the map of Figure 30.

The magnetic maps of the southwestern area have been plotted with two different intervals between contour lines. Contour lines that have an absolute amplitude 300 nT or less are drawn at intervals of 10 nT and are colored. Only positive anomalies are outside that range, and these have been drawn with black lines at intervals of 100 nT. The magnetic map of the southwestern area has been enlarged into three panels, and plotted as Figure 12, Figure 13, and Figure 14; the overlap between adjacent figures is 5 m. Since the amplitudes of the anomalies in the eastern third of that area are lower than they are farther west, this eastern panel is plotted with a closer spacing between contour lines in Figure 15, and an even closer spacing in the enlargement of Figure 16. In the northeastern area of survey, the magnetic maps are drawn with two intervals between contour lines, 50 nT in Figure 30 (this is the best view east of the stone wall), and 20 nT in Figure 31 (best for the area west of the wall).

The magnetic map of Figure 12 reveals a fault in the data near E125 N115; the magnetometer did not record values for a 5-m span there. Overhauser magnetometers, like proton magnetometers, are deliberately set to record measurements within a limited range (this reduces their sensitivity to electrical interference). In the area marked “no data” in the figure, the readings were higher than this range. The maximum anomaly that could be recorded by the magnetometer was an amplitude of about 2000 nT; however, the geological feature there causes an anomaly that probably rises to 4000 nT. While the magnetometer can be set to measure these high anomalies, that option was not suitable at this site. To measure these high anomalies, one can set the instrument to shift the allowable range according to recent readings of the magnetic field. However, if there is a very rapid change in the field (which happens where a shallow iron object is passed), this range-seeking can fail, and the range remains outside that of the measurements until the survey is stopped and this fault is corrected. If one has the choice of losing unimportant readings (highs at geological features) or important features (fainter archaeological

anomalies), it must be the geological patterns that are missed.

The final magnetic maps here have some other faults that have not been corrected, for they have little effect on the analysis of most of the measurements. These faults are caused by the guide cords not being placed at exactly the correct locations, due to the tall grass. These faults are evident because of the close spacing between lines of survey. The source of the fault is illustrated in Figure 37. If one traversing cord is shifted to the east or west from its correct location for part of a traverse, measurements on the four associated traverses will also be shifted. If there is an east-west gradient in the magnetic field, the mapped gradient will be too high on one side of the group of four lines and too low on the other side. This pattern is evident in the magnetic maps where this lateral gradient is otherwise rather smooth. Gradients that are too abrupt are apparent at the southern side of Figure 16 at E166.5 and E171.5, at the edges of the anomaly for an interesting archaeological feature near N114 (the interesting gradients in that figure near line E165 are not locational errors; these will be discussed later). Additional evidence of these east-west shifts is apparent in Figure 13 near line E132. Once these faults have been located, it would be possible to correct most of their effect. However, since the faults are not serious except where small-area features must be analyzed with the greatest accuracy, the extra time for that correction has not been taken.

A technical analysis of the magnetic measurements was done with several computer programs. The magnitude and direction of the Earth's magnetic field were needed for this analysis; the inclination of the field was determined from the parameters of the International Geomagnetic Reference Field (IGRF) for 2005 to be 72.2°. The declination angle of the field relative to grid north was estimated from a magnetic compass; the IGRF parameters indicate that magnetic north was 0.7° west of true north at the time of this survey. The magnitude of the Earth's field was determined by the readings of the magnetic base station (Figure 36), and a value of 50,350 nT was selected for the field in the southwestern area of survey.

Interesting and linear anomalies that extend in a north-south direction are apparent in Figure 16 near lines E160 and E165; these are marked with green arrows at the top of the page. A two-dimensional analysis was made of the anomaly along line E160 at N134. This anomaly was averaged across a span of 2.75 m, and it is plotted in Figure 24 with a red line. Note that this anomaly cannot be caused by an east-west error in the locations of the readings; instead of a horizontal shift, there is an abrupt change in the amplitude of the readings at this location. Bruce's computer program MagPoly found a magnetic model whose calculated field approximated these measurements; the calculations from that program are shown in Figure 24 with a blue line (a constant of 107 nT has been subtracted from all the calculations in order to shift their amplitudes to the level of the measurements). The text in Figure 24 describes the magnetic model: It is a rather thin slab that is more magnetic than the soil to the west. Because of its depth, it probably does not have a modern origin, although it must be a cultural effect. While the magnetic slab must end toward the east, this eastern edge was not located by the magnetic survey. This

could mean that the eastern edge is tapered or feathered; however, it is more likely that it is simply irregular and does not extend along a straight line.

Most of the magnetic anomalies that were found in the southwestern area were not linear, but were instead small-area bipolar anomalies. These anomalies were analyzed with Bruce's program MdMagC (Multiple-Dipole MAGnetic analysis, Constrained). This program iterates the six parameters of a dipole until the calculated field is the best approximation of the measurements. These six parameters are M (magnetic moment, Am^2), the direction of total magnetization, defined by an inclination and declination angle (I and D, in degrees), and the location of the dipole as determined by X, Y, and Z, where Z is the elevation of the dipole (m) above the ground's surface. An additional parameter must also be determined by the program, and this is the local background field near the anomaly. The parameters that were determined by this program in the southwestern field are listed in Figure 38 and Figure 39; the precision of the numbers there is greater than their accuracy.

Each of these dipolar models is located in the map of Figure 7. The estimate of mass there assumes that the relative magnetic moment of these objects is 10 mAm^2/kg; this value is typical for iron objects and for magnetic igneous rocks, such as basalt. While none of the underground objects may be either iron or basalt, this value still provides a reference for the relative masses of the actual objects.

The calculated magnetic field of these 82 dipoles is plotted in Figure 9, and this generally provides a good match to the measurements in Figure 8. The mismatch is made evident in the residual map of Figure 10. Five dipolar anomalies have poor models; these are numbers 2, 3, 5, 29, and 37. These low-accuracy models are indicated in the parameter list of Figure 38 with red numbers. While a more careful analysis of these dipoles could improve the parameters of those anomalies, that added accuracy is probably not important at this time.

Since the magnetic model of the southwestern area of survey provides a good approximation of the measurements, that model also allows a calculation of the magnetic map that could be measured with a gradiometer. This is shown in Figure 11; the calculated map is not much different if the spacing between the sensors is doubled, to a distance of 1 m. While it can be possible to calculate gradient maps directly from the measurements, small errors in the measurements would then be exaggerated.

A broad magnetic anomaly was detected on the eastern edge of the area of survey; this is marked in Figure 6, but this anomaly has not been analyzed. Most of the magnetic anomalies in the southwestern area are somewhat circular, and this suggests that compact objects are underground. Small and linear anomalies were located at two places, and these elongated anomalies are indicated with the word "line" in Figure 5 at the east side of the map, and the southwest corner of the area of survey.

In the southwestern area of survey, several similar and interesting anomalies were revealed in the eastern part of the area of survey. These were magnetic lows that were elongated north-south; they have dimensions of about 2 by 5 m. Several are visible in

Figure 16: Along line E166 near N130 and N134, and along line E156 near N134. That first anomaly is extracted to Figure 25, and the magnetic model there provides an approximation of the measurements.

A more thorough analysis was made of a magnetic anomaly that is both very distinct and which almost certainly has an archaeological origin. The pattern of this anomaly is enlarged from Figure 8 to Figure 19. The undulations on the contour lines suggest that the locations of some measurements may be north-south errors of 0.5 m; however, these cause no difficulty for the analysis. The calculated map of three dipoles provides a good approximation of the measurements; see Figure 20. Another analysis of these measurements was made with Bruce's Cprism program, and the magnetic model was a horizontal and rectangular box; the calculated field of the best-fitting model is plotted in Figure 21. A somewhat better model was possible if this box could be tilted slightly, and this solution is given in Figure 22. The commercial program, Potent (for POTENTial field analysis), was used to create this magnetic model.

The Cprism program was also applied to the analysis of anomaly F4 (dipole 58 at E175 N140 in Figure 5). The magnetic models were square boxes that were either 1.5 m or 2 m on a side. With a width of 1.5 m, the depth to the top of the box was 1.1 m and its magnetic moment was 2.9 Am^2. When the width of the box was increased to 2 m, the depth was reduced to 0.8 m and the moment was reduced to 2.4 Am^2; however, the error of this shallower model was larger. This is probably because the larger and shallower square created a non-circular anomaly; a magnetic model with a circular disk would be better than these two square models. It is most likely that this feature has a diameter of between 1.5 and 2 m; therefore its depth is about 1 m, which is 0.5 m shallower than the estimate of the depth of a compact feature, or dipole.

The magnetic map of Figure 8 reveals an interesting and broad magnetic low near E155 N135. This must be caused by natural geological strata that are deep; however, this pattern has not been studied.

A small sample of the anomalies in the northeastern area of survey were also analyzed with the MdMagC program, and their parameters are listed in Figure 32. A two-dimensional analysis was made of one of the linear anomalies; this anomaly extends north-south along line E124 and is centered near N108 in Figure 30. The measurements were averaged along columns from N106 to N110.5 and a good approximation of these measurements was provided by the calculated field of a rectangular magnetic prism having a magnetic susceptibility of 100 ppt and which has a depth range of 0.5 - 1.0 m and an east-west span from E123.75 to E124.75.

magnetic susceptibility meter

The written values were first entered into digital files, and then the readings were converted to magnetic susceptibility. Figure 40 shows how the EM38 weights the magnetic properties of soil strata by their depth. When the instrument is carried at a height of 0.3 m, the uppermost layer of the soil has the greatest effect on the

measurements, and soils to a depth of 0.3 m add further to the reading. However, magnetic soil strata that are deeper than 0.3 m underground decrease the reading of the EM38. This change in the polarity of the instrument's sensitivity confuses an interpretation: A high reading may be caused by a shallow magnetic feature, or a deep non-magnetic feature. Since archaeological features are more typically magnetic than non-magnetic, the EM38 can approximate the depth of these magnetic features, and this is beneficial. When it is operated at a height of 0.3 m, the EM38 is a detector of the destratification of the soil, and this is an archaeological effect that is worth measuring.

There are two corrections to the "conductivity" readings from the EM38 that are required so that the values will quantify the susceptibility of the soil; while these corrections assume that the soil is not stratified, that assumption cannot be avoided. The first correction adjusts the readings to values that would be correct if the instrument was carried at the ground's surface. This adjustment of the readings is simply a factor of 0.058 that is multiplied by all readings to convert them to susceptibility, in parts per thousand (ppt). If readings in full SI units are wished, these "ppt" values can be divided by 1000. The readings must then be corrected for the height of the instrument; this is done by dividing the prior values by 0.13, which is the net area under the curve in Figure 40 between a distance of 0.3 m and infinity.

The resulting map of magnetic susceptibility in the eastern part of the southwestern area of survey is plotted in Figure 17. The comparative map of magnetic field, on the right, clearly shows much greater detail. This is only partly due to the fact that the measurement spacing for that magnetic survey was smaller (0.5 by 0.2 m, as compared to 1 by 1 m spacing for the susceptibility survey). The susceptibility map shows an added variability that is probably caused by electrical interference. Unlike the magnetometer, the susceptibility meter did not detect the wire fence that is outside the north and east sides of the area of survey; however, the anomalies from the EM38 were generally faint and showed little correlation with the map of magnetic field.

During the field survey, two distinctive anomalies in magnetic susceptibility were immediately apparent; these are the two broad lows near E168 N114 and E175 N140. These lows are most reasonably caused by magnetic features that are at a depth of greater than 0.3 m. The southern anomaly was resurveyed with the closer measurement spacing of 0.5 m; the area of this further survey is outlined in green in Figure 17. The resulting map is plotted in Figure 41. The important central anomaly there is clear, but the anomalies in the map are generally elongated or striated in a north-south direction; this is a result of the faulty setting of zero susceptibility during the field work.

These striations were studied by calculating the average reading along each north-south column; these averages are plotted in Figure 42 with red lines (The central anomaly was excluded from the averages of the original measurements). By adding or subtracting different constants from all of the readings on each north-south line, the averages in the resulting map were forced to a smooth and reasonable curve, plotted in Figure 42 with a blue line. A similar correction was applied to the original susceptibility survey, and the

resultant map is plotted on the left side of Figure 17.

resistivity meter

The written values of resistance, in ohms, were first entered to computer files, and then they were converted to resistivity, in ohm-m. This conversion is the same as that applied to the Wenner array:

Resistivity = (twice pi = 6.28) x (electrode spacing = 1 m) x (resistance, ohm).

These resistivity values are plotted in Figure 33. There is generally little correlation from one line to the next parallel line; however, the three coinciding highs at N112.5 may reveal a linear feature that extends east-west.

The electrical resistivity of the soil ranges between 1000 and 7000 ohm-m; these overall high values mean that there is a large fraction of sand in the soil. The highest readings probably locate where bedrock is shallow, although it is possible that the soil at those locations is pure sand or gravel, without silt or clay. The rather uniform and low readings on the east side of the stone wall suggest that bedrock could be deep there.

From these factors, it can be estimated that the resistivity of bedrock here could be about 10,000 ohm-m, while the average resistivity of the soil could be about 1500 ohm-m. If one assumes that these are the exact parameters of rock and soil, it is possible to calculate the depth to bedrock. Figure 44 shows how a reading of resistivity may be converted to this estimate of depth. The two resistivity profiles on the western side of the stone wall can then generate the crude topographic map of bedrock that is plotted at the left side of Figure 29. In most parts of the survey area northeast of the church, bedrock is probably deeper than 1.3 m

Findings of the Geophysical Tests

The most important results of the surveys in the area southwest of the church are mapped in Figure 5. Moderately small features are located with asterisks; lines and rectangles mark larger features. The feature at F1 (E168 N115) was detected very clearly and the rectangle there approximates the extent of this feature; its depth and volume could also be estimated. Feature F4 (E175 N140) may be similar to feature F1, although F4 is smaller and more circular. The rectangular patterns that are dashed in Figure 5 may reveal elongated holes that have been dug into the topsoil; these may be modern features, for they appear to be shallow. The patterns that are marked with lines having tick marks along their length in Figure 5 locate abrupt soil boundaries; these features appear to be at a depth of about 0.5 m. Some of these boundaries (the ones near E165) appear to locate the edge of a recent excavation; no certain explanation has been found for the boundaries near E160. The curving lines toward the west trace a ridge of shallow bedrock; the pattern there is not what was expected.

The main findings of the test that was made northeast of the church are plotted in Figure 29. Distinct linear features that tend to be oriented north-south were very apparent on the eastern side of the stone wall. These linear patterns are not caused by bedrock,

for rock appears to be rather deep on this side of the wall. Instead, perhaps the patterns locate bands where the soil was removed to different depths; the lines could mark ridges between scraped areas. These patterns were not found on the western side of the stone wall; bedrock on that side was found to approach the surface in the northwestern part of the area of survey.

Further details about these findings are given below.

southwest of the church

The most interesting findings in the southwestern area are marked with an F in Figure 5, where F stands for finding or feature. Feature F1 is enlarged in Figure 18. A broad object, with dimensions of about 3.3 by 1.4 m was detected here by both the magnetometer (Figure 19) and the magnetic susceptibility meter (Figure 23). This feature is moderately deep, although probably closer to a depth of 0.5 m than 1.0 m. It is likely to be a fired earth surface and it could be a large hearth. However, it is not impossible that it is a layer of gravel, with the stone being igneous or metamorphic. The evidence for a fired surface was found by an analysis of the magnetic map; the magnetic field within this feature is in a direction that is close to that of the Earth's present field, although the magnetic direction in this feature is west of the Earth's field.

Feature F4 is near the northeastern corner of Figure 5, at E175 N140. The object at this location could be similar to that at F1, and both are likely to be fired. Features F1 and F4 were the only features that were detected by both the magnetometer and the magnetic susceptibility meter (These findings can be compared in the map of Figure 17). One interpretation for Feature F4 is listed next to its locating asterisk in Figure 5. The number 58 is just a sequential identifier for this particular object. The values that are listed below that identifier give an estimate of the mass of a compact object (387.2 kg) and its depth (1.5 m). Both of these values are almost certainly too large; an analysis of a magnetic map provides valuable estimates of these parameters, but they are much more likely to be overestimates than underestimates. If the object at F4 is broad, rather than small, the depth would be less. For example, if the object is about 1.5 m in diameter, its depth would be about 1 m, and this is more reasonable than a depth of 1.5 m. Furthermore, the depth must be shallower than about 1.5 m underground in order for the feature to have been detected by the magnetic susceptibility survey. The estimates of the masses of features here assume, for convenience and consistency, that they are composed of iron or a magnetic stone like basalt. If the features instead are composed of in-place fired earth, then the estimates of mass should be increased by a factor of ten. If the features are composed of many broken fragments of ceramic or other fired soils that have been disrupted or broken up, then these masses should be increased by a factor of one hundred.

A comparison of Features F1 and F4: Both are probably composed of fired earth and both have about the same quantity of magnetic material. Feature F1 is elongated and has about twice the area of Feature F4. Since they both have the same amount of

magnetic material, F4 could be thicker than F1, or Feature F4 may simply contain magnetic minerals that are more magnetic per unit of volume. Feature F4 is about 0.4 m deeper underground than Feature F1. On a technical note, the magnetic low from Feature F1 is distinct, while the low from Feature F4 is relatively weak; it is possible that the edges of Feature F1 are more abrupt than are the edges of Feature F4.

Feature F3 (in Figure 5) is a magnetic boundary that extends in a north-south direction along line E160.5 near N134. The soil at a depth of about 0.5 m is more magnetic on the east side of this line than on the west side. For a closer look at the magnetic map of this feature, see Figure 16; Feature F3 is just below the green arrow on the left side. While the magnetic character of this feature is well-defined, its archaeological importance is not known. Its depth suggests that it may not have a modern origin. Only one side of this feature has been detected; the other boundaries are diffuse or irregular and cannot be located in the magnetic map.

There is another feature that is almost identical, and this is found 8 m to the south; see the magnetic map of Figure 16, or the interpretation of Figure 5. While a detailed analysis was not made of this southern feature, its depth is probably about 0.5 m also. However, this southern feature marks a boundary where the soils are more magnetic on the west side of E160, rather than on the east side.

Other and similar boundaries are marked in Figure 5 near line E165. The magnetic map of Figure 16 shows these anomalies, and also another possible one near N132. The magnetic boundaries near E165 probably locate one of the edges of an excavated trench that crossed this survey area. It is surprising that no parallel feature is found at a distance of 3 m (the width of the trench) to either the east or the west. The invisibility of that edge of the trench must be due to the way the soil was filled back into this trench (perhaps it was shoved into the trench with power machinery, rather than thrown in with shovels).

Feature F2 suggests that the archaeological trench extended to the east from E165, rather than to the west. This feature is located near E166 N130, and its magnetic map is enlarged in Figure 25. This feature, and a similar one that is 5 m to the north, appear to be caused by the naturally-magnetic topsoil in this region having been replaced by (probably) less magnetic subsoil. This is likely a modern feature, and it could simply be a result of the change in soil stratification when the trench was filled.

Could the magnetic boundaries near E160 also be caused by that former excavation? They are clearly too distant to be the other edge of the trench. However, if the soil from the trench was piled along a ridge to the west of the trench, then the boundaries near E160 might, in principle, be caused by remanent wedges or lenses of soil that did not go back into the trench when it was filled. Unfortunately for this interpretation, the features along line E160 truly appear to be too deep to be caused by soil left at the surface. While the source for these features is not known, this study does show the large amount of work that is needed to study the (possibly) unimportant patterns caused by former excavations. While excavations that precede a geophysical survey are extremely valuable in suggesting the depth and character of archaeological features, they do

complicate the analysis of a later geophysical survey!

Additional magnetic “holes” are located in Figure 5 with broken-line rectangles. These are less likely to have a modern origin, and these may reveal shallow archaeological features. While these rectangular patterns have a dimension and extension that is typical of grave shafts, their north-south orientation makes graves an unlikely cause for these anomalies. Since the topsoil here is probably more magnetic than the subsoil, a refilled pit can be detected as a magnetic “hole” also; this is because that topsoil may be put back into the excavation at a greater depth and the upper layer of soil may now be less magnetic that the surrounding natural soil.

The western trench that crossed this field was located near E124. The magnetic map detected no trace of that filled trench; this is partly due to the fact that geological features caused large anomalies in that area, and these may have hidden the fainter anomaly of the fill soil.

There is another question relating to the prior excavation in this area. Was feature F1 exposed in the eastern trench? It was clearly very close to that trench, and it is possible that the trench exposed its upper surface. If that feature has already been examined in an excavation, then a re-analysis of this geophysical survey could be done, and this might allow a better understanding of the part of feature F1 that has not been unearthed.

Many other small-area features were located by the magnetic survey that was done in the southwestern area, and Figure 5 locates the most important of these. If features have a width of 1 m or more, their depths are likely to be too deep in the interpretation of Figure 5. It is for this reason that features to a maximum estimated depth of 2 m are included in this figure; some of the features at that maximum interpreted depth may be only about 1 m underground.

The curving lines in Figure 5 trace where ridges of bedrock are likely to be found; no attempt was made to determine the depth to the top of bedrock with accuracy, but this depth may be greater than 2 m. The interpretation of the magnetic bands is fairly certain, but they do not fall along the paths that were expected. A shallow ridge of soil extends north-south across about the middle of the area of survey; this ridge is faintly visible as a light color in the aerial photograph at the upper right corner of Figure 3. These aerial and topographic patterns are quite different from the findings of the magnetic survey. The results of the excavation in the western trench may reveal which of the linear patterns correctly locates shallow bedrock.

The map of Figure 6 reveals additional objects that were detected, but these may have less archaeological importance than those in Figure 5. The objects in Figure 6 are either quite deep, or are more likely to have a modern origin. This modern origin is suggested where objects are very shallow. This recent origin is also suggested where small-area magnetic anomalies are primarily lows, or where the orientation of the magnetic field inside the feature is very distant from the direction of the Earth’s field. These anomalies are likely to be caused by steel artifacts that have been lost. Since

interpretation is not perfect, it is possible that some of the findings in Figure 6 do have archaeological importance.

The anomaly of object 5 (at E128 N119) in Figure 6 is unique in the area. A huge magnetic object is almost at the surface there; this must be a modern steel artifact.

northeast of the church

The findings of the geophysical test that was done northeast of the church are plotted in Figure 29. That summary is not adequate for showing the extreme difference that was found on either side of the stone wall that is near E120. The magnetic maps of Figure 30 and Figure 31 are better for showing the abrupt change in the patterns at the stone wall, which is located at the break between the two sections of the map. It is also valuable to compare Figure 31 with Figure 8 (a magnetic map of the southwestern area). The amplitudes of the anomalies in the eastern section of the northeastern area are much greater than the amplitudes of the archaeological anomalies that were found in the southwestern area of survey.

One should first suspect that the strong anomalies in Figure 31 must be caused by magnetic bedrock. However, bedrock appears to be deeper than 1 m in that eastern area while an analysis of the magnetic anomalies suggests that the source is about 0.5 m underground. Therefore, the strong and linear magnetic patterns in the eastern section must be caused by features within the soil.

It is next necessary to estimate if the linear magnetic anomalies east of the wall may be caused by ridges of soil there. The topography there is indeed complex, with rises and falls of about 0.5 m in some areas. While no north-south ridges were apparent at the surface, this area should be examined for linear ridges that match the pattern and location of the linear anomalies in Figure 29. The most apparent ridge in this area was the fragment of a circle that is found crossing the eastern section from N100 to N110; this circular ridge has not created a magnetic anomaly.

It appears that the source of the linear patterns is therefore underground in the soil. No evidence suggests whether these soil contrasts were part of the original construction of the ancient mound, or whether they are a result of the recent leveling of the mound.

In addition to these linear features, about 16 compact objects were located by the magnetic survey; these are marked in Figure 29 with asterisks (if they were analyzed) or X symbols (if they were not).

The measurements of electrical resistivity in the northeastern area allowed estimates of the depth to bedrock. Figure 29 shows that this rock appears to be most shallow toward the northwestern part of the survey area. An approximate topographic map there reveals that bedrock quickly becomes deeper toward the southeast.

Comparison with the Radar Survey

A comparison of the findings of all of the surveys in the southwestern area will

enable a greater knowledge about what is underground. While a report from the earlier radar survey is not available now, we are fortunate to have the time slices of the radar images, and these are in a *.tif format that is readily viewed.

In the southwestern area of survey, this geophysical test applied the grid and corner stakes that were set up by an earlier radar survey of this area. While it is reasonable that locations from this test should have a maximum error of 0.5 m relative to the findings of the radar survey, it was found necessary to shift the radar data to the west by about 1 m relative to the magnetic interpretations for the best correlation between the findings.

While a better comparison of the data can be made later, an approximate review of the similarities and differences was made by simply viewing the plan maps of the radar echoes on a computer display, and then adjusting the size of those maps to match paper prints of the interpretations of this geophysical test; these paper prints were set on the computer's display and aligned with the radar map. Correlations were sought by stepping through the time slices of the radar data. A better comparison can be made with a digital overlay of the interpretation maps of this test on those radar images.

Correlations were rare. If it were not for several correlations that are clear and certain, one might suspect that the surveys were done in different locations. This lack of correlation was welcome. If the same findings resulted from both surveys, one of them would have been a waste of time and money. However, it can sometimes be very difficult to justify why a particular feature may be detected by one instrument and not another

The findings of radar and magnetic surveys are almost always quite different; this is a major reason why it can be beneficial to try both techniques. A radar survey is usually a detector of horizontal interfaces, while a magnetic survey is generally a detector of volumes and abrupt edges. While a radar survey can detect magnetic contrasts, it is best for revealing contrasts in the conductivity or permittivity of features; this is also part of the reason for the difference in the findings of these surveys.

Comparisons between the findings of the surveys are listed below; the depths listed for the radar data are those in the file names of the time slices.

The distinctive feature F1 (Figure 18 at E168 N114, at a depth of 0.5 - 1.0 m) was detected by the radar in the same area at a depth of 0.7 - 0.9 m.

The linear boundary near line E165 (Figure 16, at a depth of 0.5 m) was detected by the radar with a high echo amplitude to the east at a depth of 0.45 - 0.65 m.

Magnetic object 71 (Figure 7 at E157 N114 at an estimated depth of 2.6 m) was strongly detected by the radar in the depth range of 0.7 - 1.2 m. The overestimate of the depth of this feature by the magnetic survey suggests that it is a broad feature. The amplitude of the radar echo from this feature was much stronger and clearer than the echo from feature F1.

Magnetic object 14 (Figure 6 at E173 N119.5 at a depth of 0.4 m) was probably detected by the radar at a depth of 0.45 - 0.55 m. The nearby magnetic object 26 (Figure 5 at E173.4 N117.8 at a depth of 0.6 m) was also probably detected by the radar, at a

depth of 0.2 - 0.4 m.

Distinctive magnetic feature F4 (Figure 5, object 58 at E174.9 N140.1 at a depth of 1 - 1.5 m) was not detected by the radar. The linear boundaries near E160 in Figure 5 were also not revealed by the radar. None of the rectangular magnetic lows that are marked in Figure 5 are correlated with findings from the radar.

There are locations where a distinct radar echo is about 1.5 m distant from an object that was detected by the magnetic survey; these distances are too great to be caused by a locational error, and so different features must have been detected by the surveys.

There are dozens of locations where the radar images show a clear echo, but where this geophysical test found nothing. Also, broad-area textural contrasts in the time slices from the radar do not appear to correlate with the magnetic finding of shallow bedrock along the curving lines in Figure 5.

Suggestions for Further Work

Archaeological excavations may be next. The findings of this geophysical test may aid the selection of some locations for those small-area excavations. Perhaps some excavations will be sited where an archaeological feature is most certain; feature F1 (Figure 5 at E169 N114) is a geophysical finding in this category. Some excavations might be placed where one geophysical instrument detected a feature, but another did not; these excavations may reveal the relative success or suitability of the different geophysical instruments. Some excavations must deliberately be located where none of the geophysical surveys found anything of interest; these excavations will reveal what important features will remain undetected by any survey.

The source of a geophysical anomaly will generally be visible in an excavation, but not always. Perhaps the source is deeper underground, or within the side wall of an excavation. Perhaps the source has a diffuse boundary or otherwise shows no contrast in color or soil texture. There still may be an archaeological feature that is invisible to the eye. Geophysical tests in an excavation can solve these difficulties.

A geophysical interpretation, like that in Figure 5, provides a good guide to the central location of features; their lateral extent may be more uncertain. For the greatest likelihood of finding a feature in an excavation, the area of excavation should include the location that is marked with a symbol in Figure 5 (numerical coordinates for most of the findings are in Figure 38 and Figure 39). If a small excavation might not reveal the soil contrast at a feature, that excavation can generally be extended in any radial direction to search for the contrast at the boundary of the feature.

Should excavations in the southwestern field indicate that the magnetic survey was particularly good for locating archaeological features, it is suggested that another magnetic survey be done in that area when the grass has been cut. This better survey will allow locations to be more accurate, and that will enable a more detailed interpretation of the data. This test has also shown that a magnetic survey with a gradiometer will reduce

some of the interference from deeper geological features (see Figure 11); with a gradiometer survey, features closer to the ridges of bedrock will also be clarified.

It would be valuable to understand the magnetic stratigraphy of the soil at this site better; with a better knowledge of this, the interpretation of magnetic maps would be improved. These additional tests could be done on the sides of open excavations, or it might be possible to make them in bored holes (if the soil was not too stony). It would be good to measure the magnetic properties of stones in the area. The magnetic map that was measured adjacent to the stone wall shows little effect from those stones; perhaps some stones here are not as magnetic as was anticipated.

Some further resistivity tests would furnish a better understanding of the archaeology and geology at the site. A few resistivity soundings in the southwest field could determine the thickness of soil over bedrock. Since Feature F1 (Figure 5 at E169 N114) has a location and importance that is already known, it would be valuable to understand the resistivity character of this feature. That could best be determined with a resistivity pseudosection across it; with this technique, the cross-section of the soil is approximated.

The known tunnel below the parking lot south of the church was invisible to an earlier radar survey. Further geophysical work should be done so that the path of the tunnel can be estimated where it is not yet known. First, measurements of the electrical conductivity of the soil in that gravel-covered parking area should be made, either with a conductivity meter or a resistivity meter. This test will reveal whether the soil there has become conductive due to de-icing salts having been placed there in the winter; these salts would attenuate a radar signal and that could explain the earlier failure. Whether or not the soil is conductive, a resistivity pseudosection could be measured across the known or likely path of the tunnel as a test of its detectability. An informal test was made in June over the parking lot with a magnetometer; however, there were so many cars in the lot then that this test was indecisive. A better test could be done on a day when the cars were distant.

Conclusions

It appears likely that a magnetic survey is very suitable for finding archaeological features that are composed of fired earth at this site. While geological features will be very apparent in some areas, these are generally deep enough that they do not cause any severe difficulties. The magnetic maps suggest that there are rather few large and naturally-placed boulders in the soil; since the anomalies of these boulders can mimic archaeological features, their rarity is important. However, there are probably still enough magnetic stones in the soil that it may be impossible to identify small earthen features, such as trenches and refilled pits, with a magnetic survey. However, that conclusion will remain uncertain until the magnetic parameters of earthen features and rock at the site have been measured.

Feature F1 (Figure 5 at E169 N114) has the dimensions and magnetic character

that are possible for a hearth. It is reasonable that Feature F4 (Figure 5 at E175 N140) might also be a hearth. It is possible that object 71 (Figure 6 at E157 N114) is a hearth also, although this feature is unusually deep. Any of these features might instead be cooking pits; at a later time, further geophysical work might allow a distinction between these types of features.

It is not impossible that post holes have been detected by the magnetic survey; however, the interpretation of the survey has not been able to identify any anomaly as being caused by a refilled post hole. Identification is much more difficult that detection; this is because many small features can cause the same geophysical anomaly as a post hole.

The most certain identification of the location of a house would be the oval trench that was dug around it; none have been revealed by this test. This does not mean that these trenches and houses are not here; it simply means that the stratigraphic complexity of the site has too great for these moderately-small features to be isolated and identified. It is likely that future surveys will also fail to be certain in their identification of these historic remains of buildings. While this will make the findings of a geophysical survey less certain than is wished, the capability for locating some features may be a valuable guide to the locations of some houses, and this can economize on the cost and damage of excavations.

The geophysical tests in the northeastern area found an astonishingly large contrast in the soils on either side of the stone wall that is there. The bands of magnetic soil that were discovered on the east side of the wall could be rather recent, or they might have originated with the construction of the Viking-age mound. Test excavations in this northeastern area might be extended in an east-west direction so that these linear features will be crossed. Perhaps archaeological excavations at other mounds have already shown the cause of these patterns, which could either be contrasting soils that were deposited during mound-building, or even lines of graves. No patterns that suggest separate shafts of horizontal graves were detected by this test.

It was proper that the grass in the southwestern field was not cut for this test. That cutting could have delayed this test or caused other difficulties at the site; furthermore, the magnetic survey may have failed to be useful. Since the magnetometer appears to be an excellent instrument for this site, it is recommended that future areas for survey have the grass cut; this will allow better magnetic maps that will provide richer information.

Excavations that are made before a geophysical survey can aid that geophysical work by revealing the character and depth of important archaeological features; this information can allow a geophysical interpretation to be more certain and it can even allow geophysical descriptions of the findings to be replaced by valuable cultural identifications. However, those excavations, refilled or not, can confuse a later geophysical survey by creating many additional and unwanted anomalies. Perhaps tools were lost in the muddy bottom of an excavation. Perhaps nails remain that marked the edges or faces of the excavation. The soil that went back into the excavation was destratified from its earlier

pattern, and perhaps not all of that soil was returned to the hole, but was left at an unknown location on the surface. All of these archaeological modifications can be detected by a later geophysical survey.

At Avaldsnes, the locations of recent archaeological excavations are known precisely. At a later time, those locations and findings can be compared carefully to the discoveries of this geophysical test. It is possible that photographs or recollections will allow the locations of piles or ridges of excavated soil to be approximated, and this might allow a better understanding of the possible importance of some geophysical findings.

The electrical resistivity of the soil at this site is very high, and this allows a high resolution radar to profile to a depth of a few meters into the soil. An evaluation of the radar test in the southwestern area will determine whether geological or archaeological features predominate or are confused with each other; this is the same decision that must be made for the magnetic survey.

This test has suggested that there is a relatively large amount of electrical interference at this site to a conductivity meter, such as the EM38 operating in either its conductivity or susceptibility modes. A susceptibility survey appears to have no advantage compared to a survey with a magnetometer.

While there will be difficult challenges for future geophysical surveys at Avaldsnes, this important site deserves a careful archaeological study and geophysical exploration will be able to aid this study by reducing cost and unnecessary excavation.

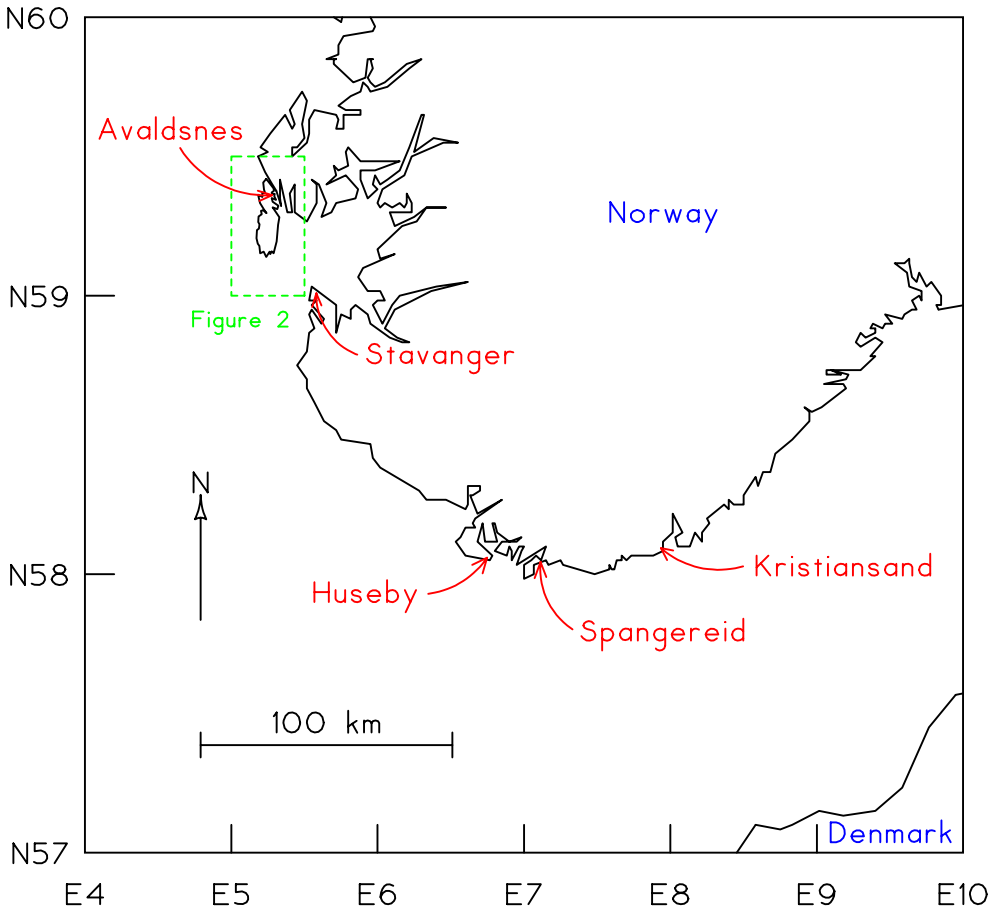

Figure 1: Southwestern Norway and the location of Avaldsnes. It is northwest of the city of Stavanger at geographic coordinate E 5° 17' 29, N 59° 21' 21". The dashed-line rectangle locates the topographic map of Figure 2. Except for the island of Karmøy, the coastline here is from the coordinates of the Micro World Database 2.

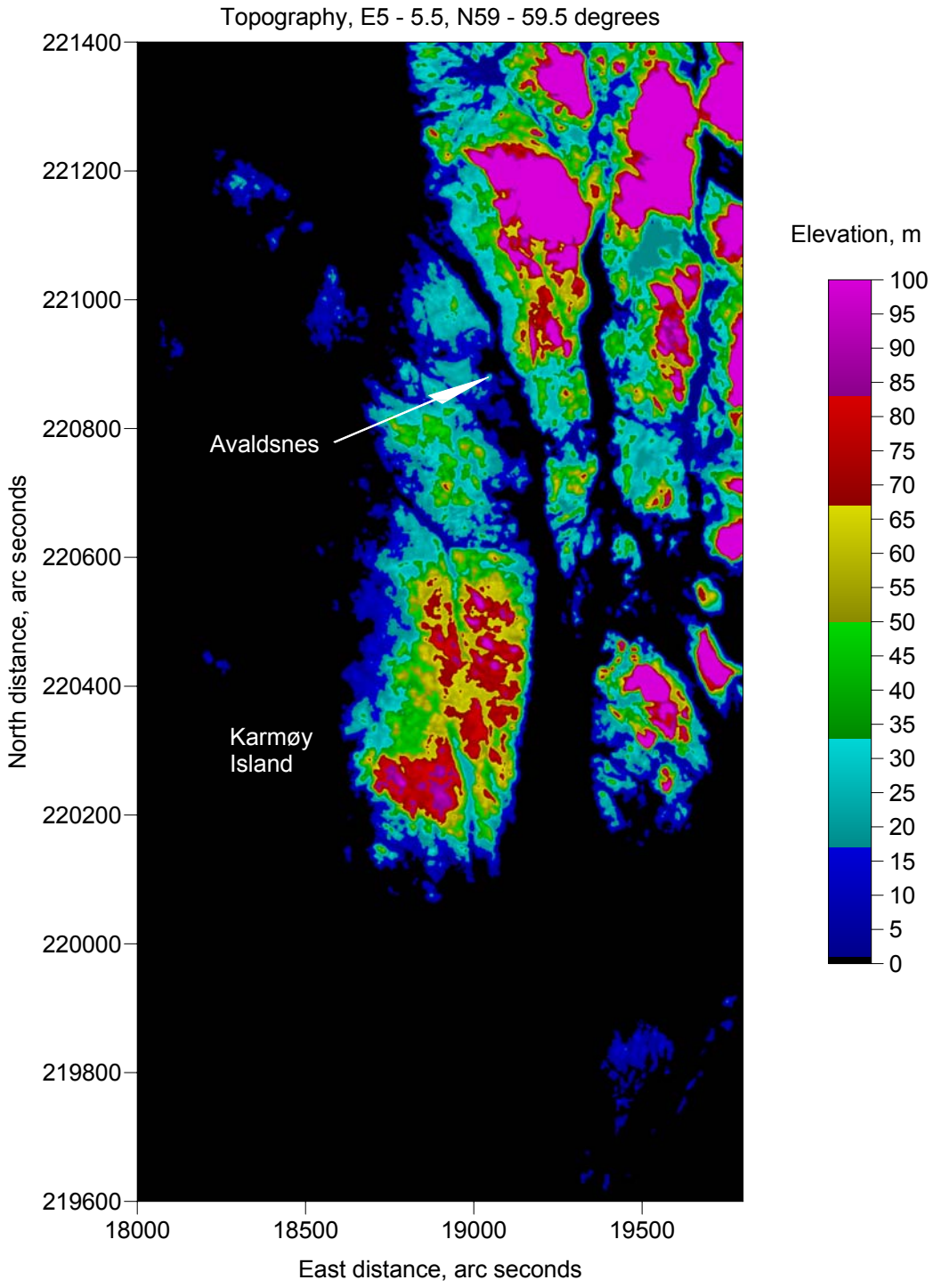

Figure 2: A topographic map of Karmøy Island. Hills are found in the southern side of the island, while the area near Avaldsnes is relatively flat and low. The site is at an elevation of 25 m; it is on the edge of a cliff that overlooks a narrow gap between the island and the mainland. Elevations in this map are from the Shuttle Radar Topography Mission; they were measured at intervals of 3 arc seconds. The ground dimensions of this map are about 29.3 km east-west and 55.6 km north-south.

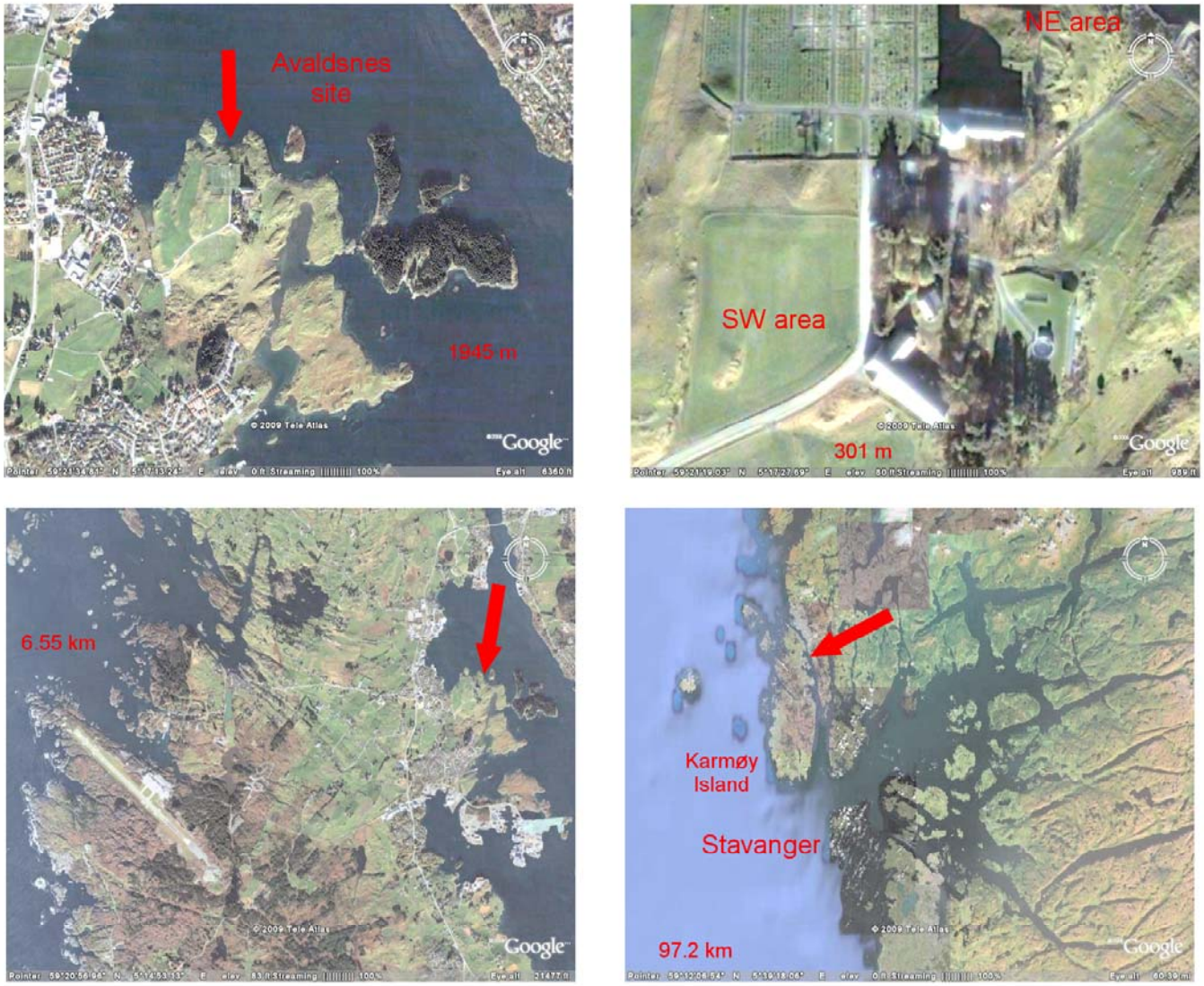

Figure 3: Aerial views of Avaldsnes. The photo at the lower right shows the largest area, and it includes all of Karmøy Island. Going clockwise, the photographs are greater enlargements. The numbers in the photographs list the width of each illustration on the ground. The greatest enlargement, at the upper right, shows the historic church at the north (casting a long shadow); the underground museum is on the right. These geophysical tests were done in two areas: Northeast of the church, next to the cemetery; and southwest of the church, in a grassy field.

Figure 4: The grassy field southwest of the church. This is a view to the northwest from the paved road that leads to the church. The southern end of the geophysical grid is marked by a line of red-and-white flagged stakes that extend to the left from the road. The northern end of this grid is next to the wire fence at the far end of the field; the grid was aligned with that northern fence. The grass in this field was about 0.6 m tall at the time of this field work; many of the traverses that were walked during the survey are visible by the lines in the grass.

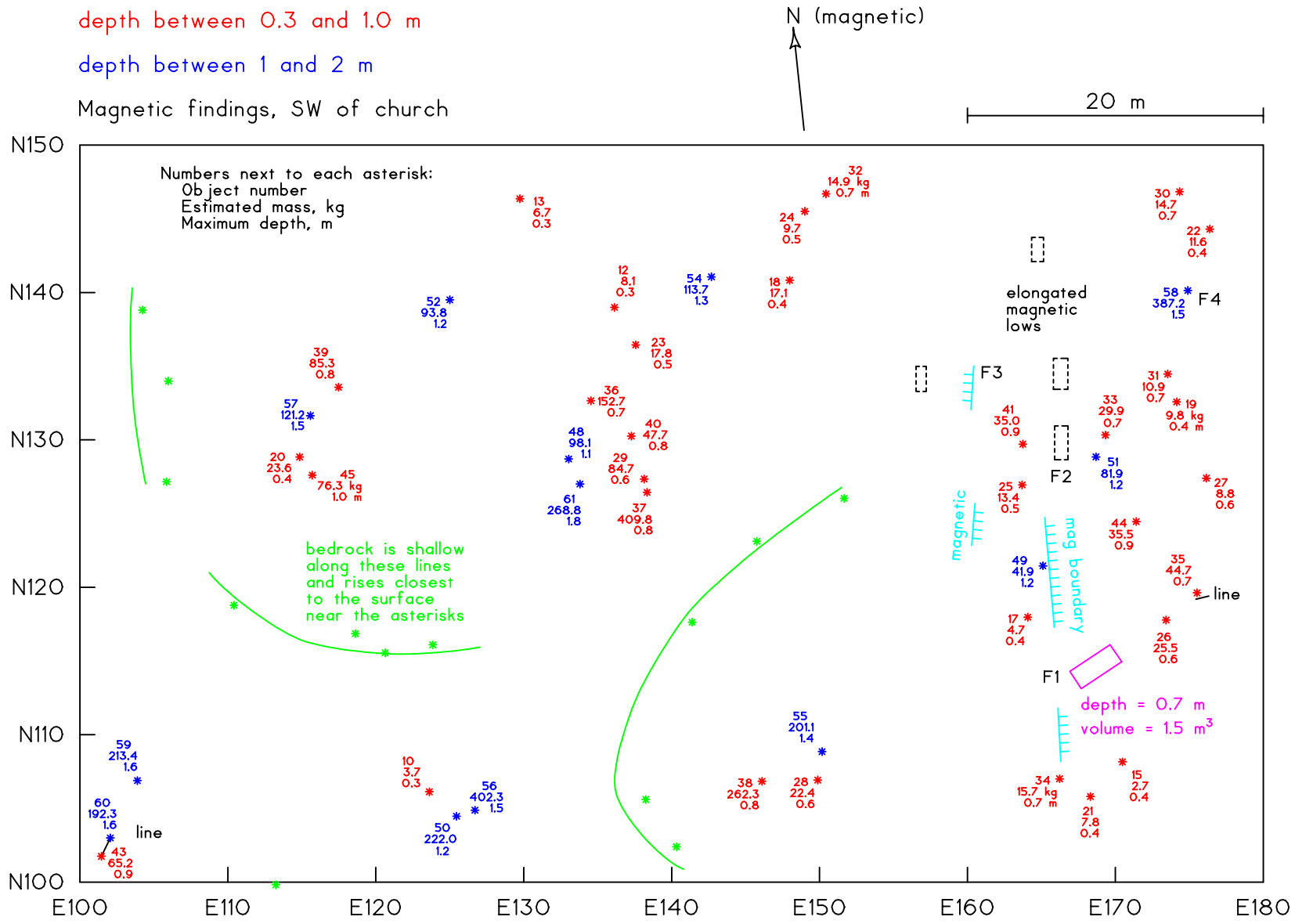

Figure 5: The major findings of the magnetic surveys in the southwestern area. Objects that are relatively small or compact are marked with asterisks. In the eastern part of the area of survey, larger features are located with lines and rectangles. Ridges along bedrock are shown with curved green lines.

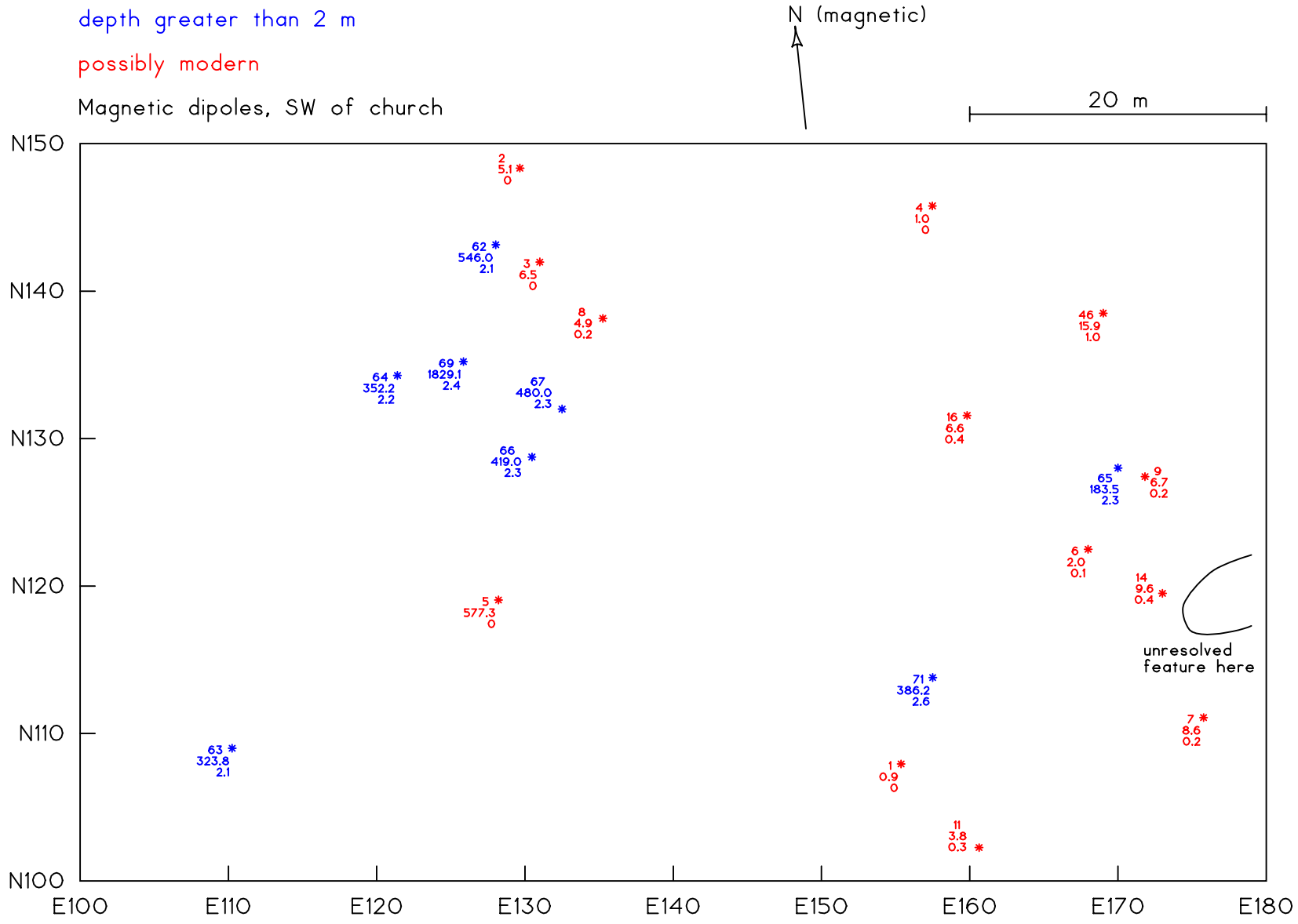

Figure 6: Findings that are less important. These features are more likely to be modern or to have a geological origin. In addition, one broad anomaly was found at the eastern edge of the area of survey, and this has not been analyzed.

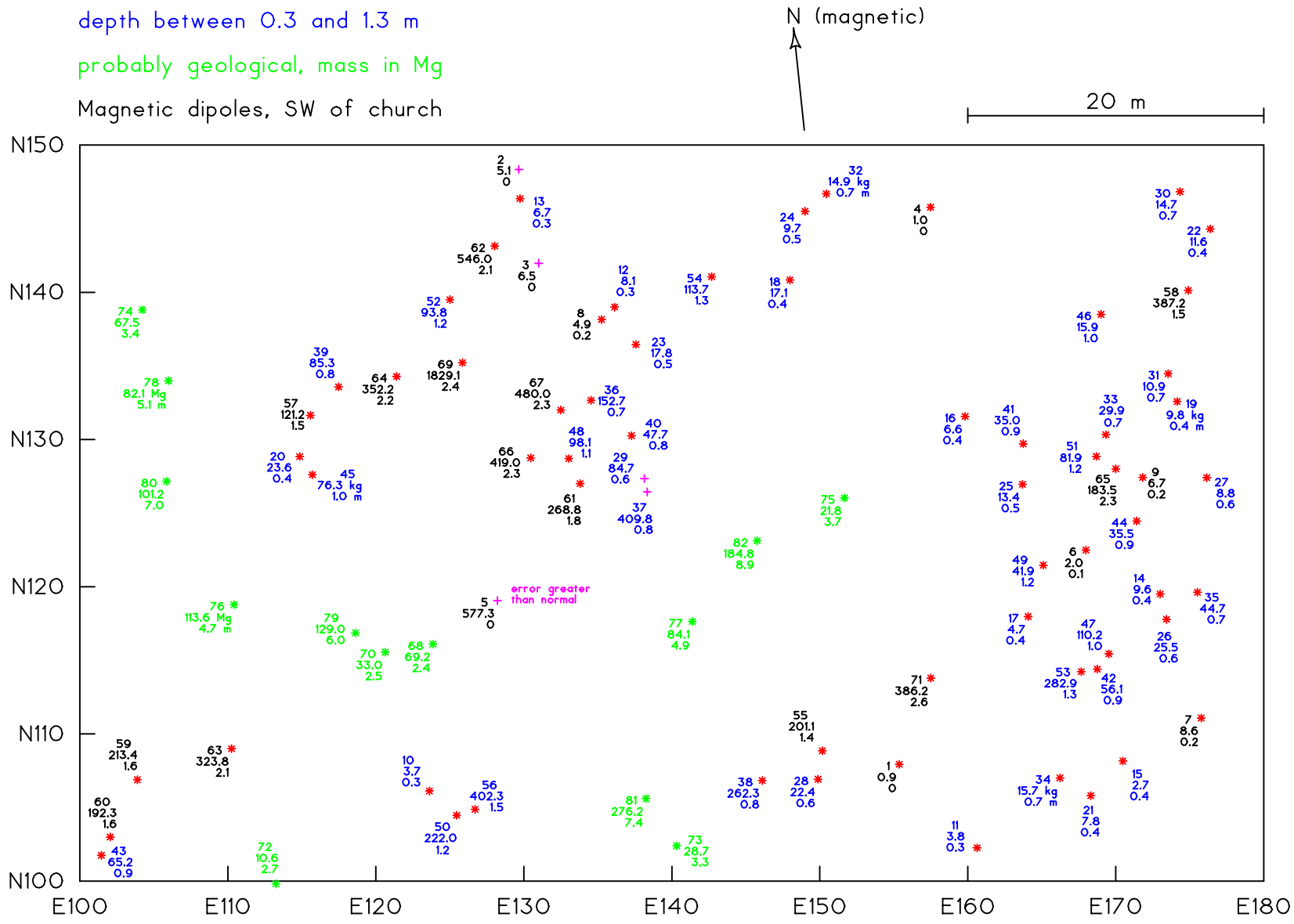

Figure 7: All of the compact objects that were analyzed. The numbers next to each * or + symbol list the object number, the estimated mass, and the estimated depth. These estimates of mass and depth are more likely to be too large rather than too small.

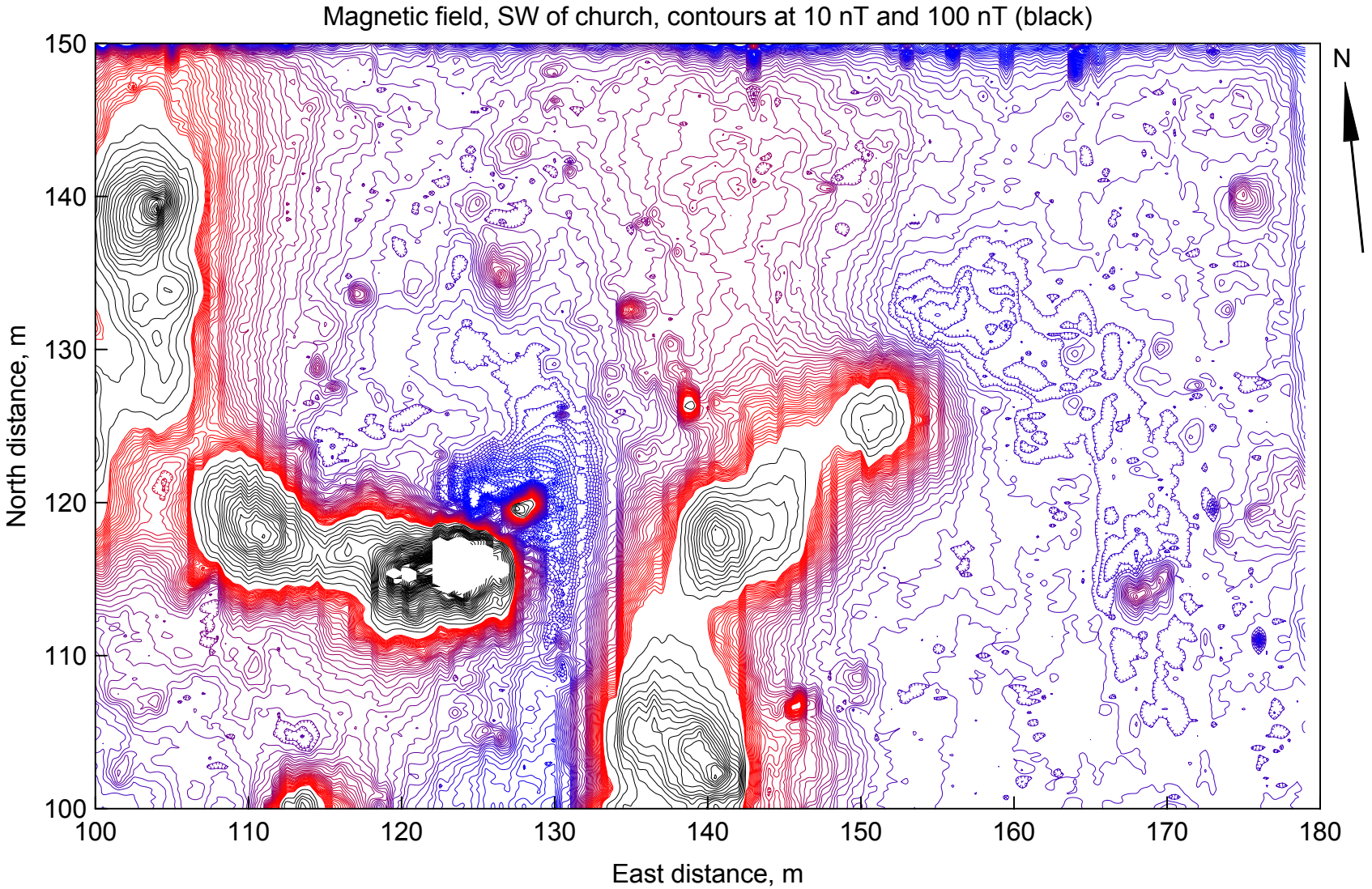

Figure 8: The magnetic map of the southwestern area. Magnetic highs are colored red, although extreme highs are black and contoured at intervals of 100 nT. Magnetic lows are blue, and the lows at the north and east side of the area are caused by fencing wire.

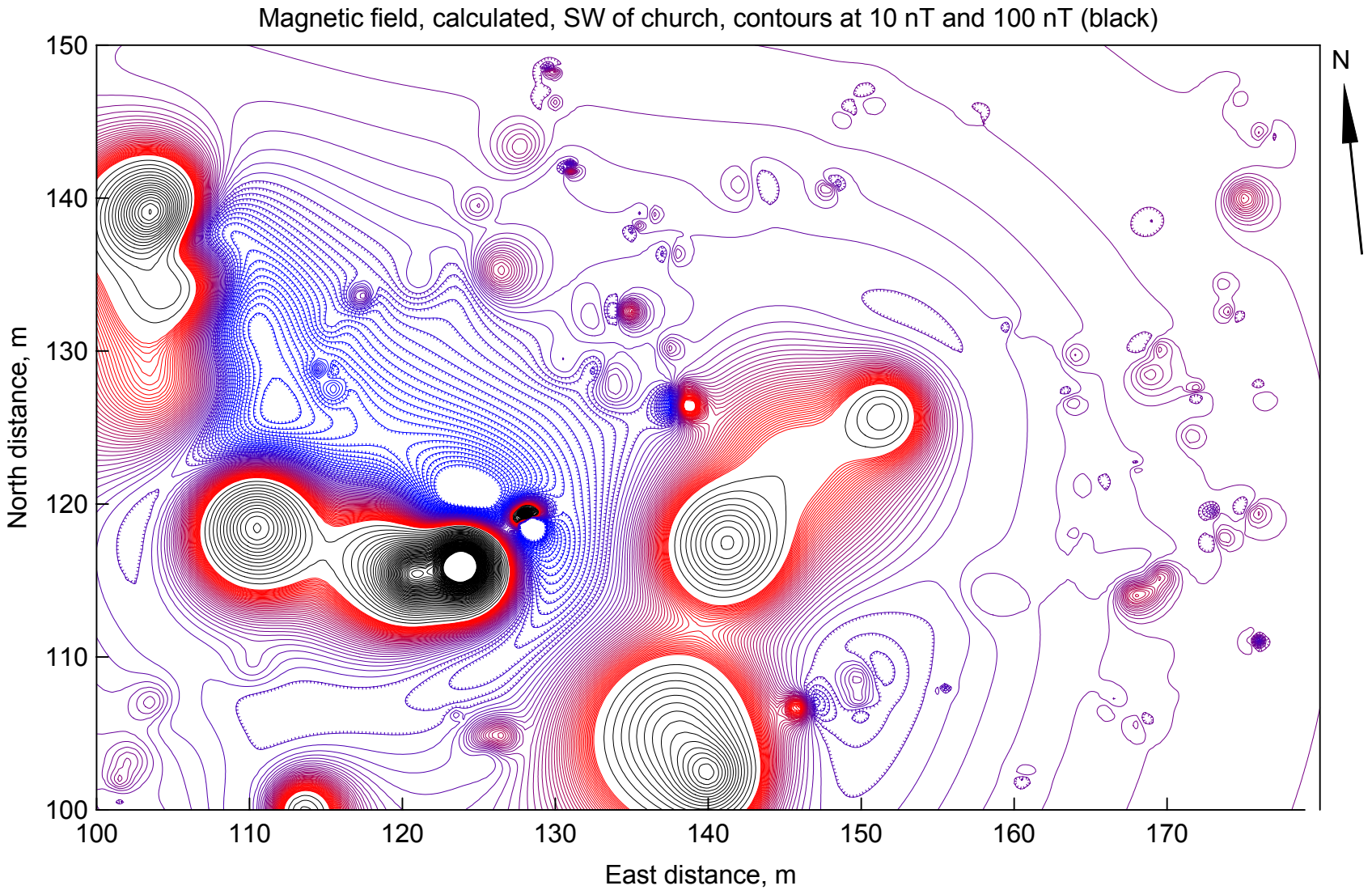

Figure 9: A calculated magnetic map. This shows the magnetic field of the dipoles that are plotted in Figure 7 and listed in Figure 38 and Figure 39. Since the calculations show patterns that are generally similar to the measurements, the parameters of the dipoles are approximately correct.

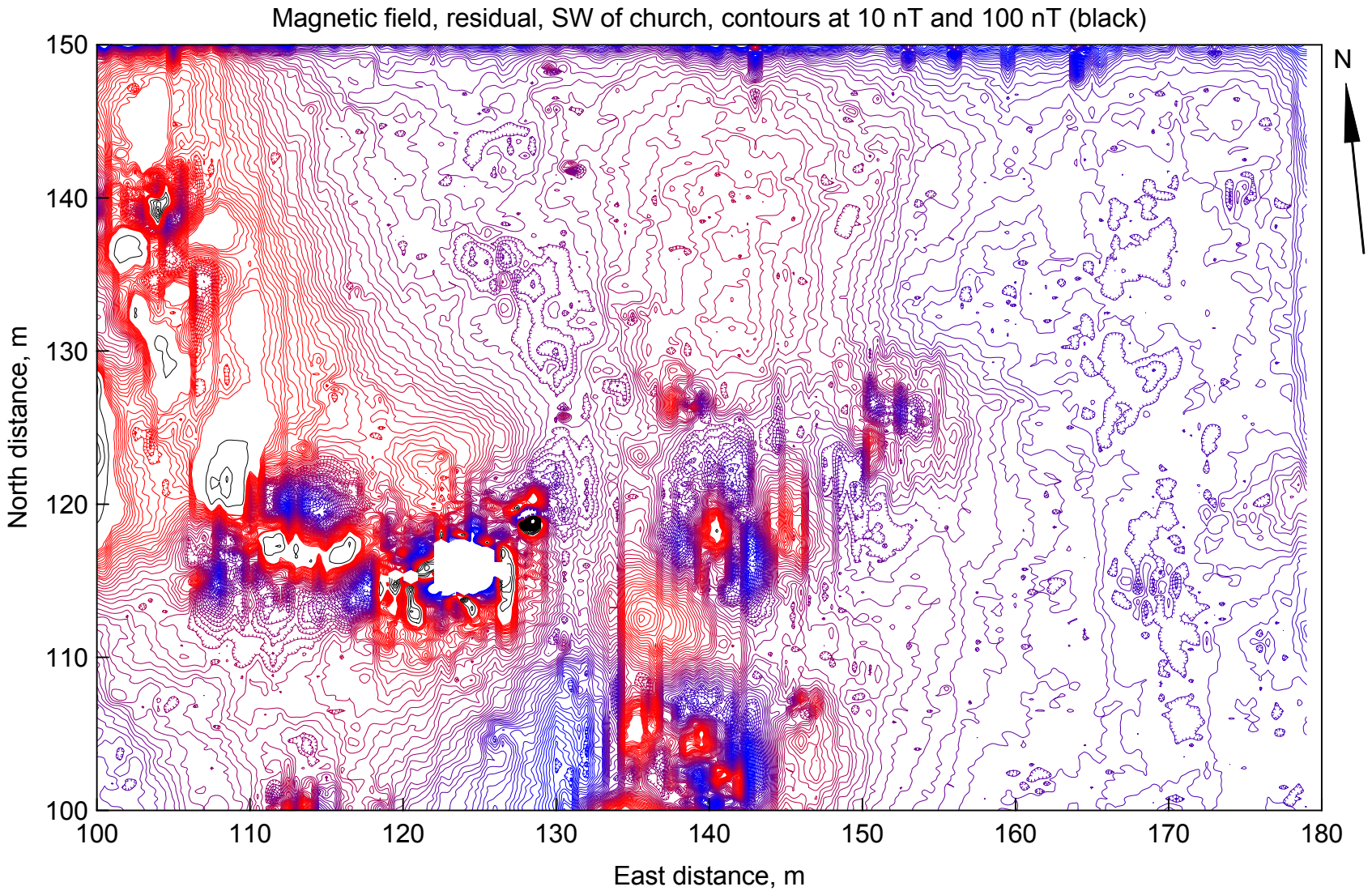

Figure 10: A residual magnetic map. This is the measurements of Figure 8 after the calculations of Figure 9 have been subtracted. If the analysis was perfect, there would be no patterns in this map. However, the anomalies are generally attenuated and this indicates their approximation by the calculations.

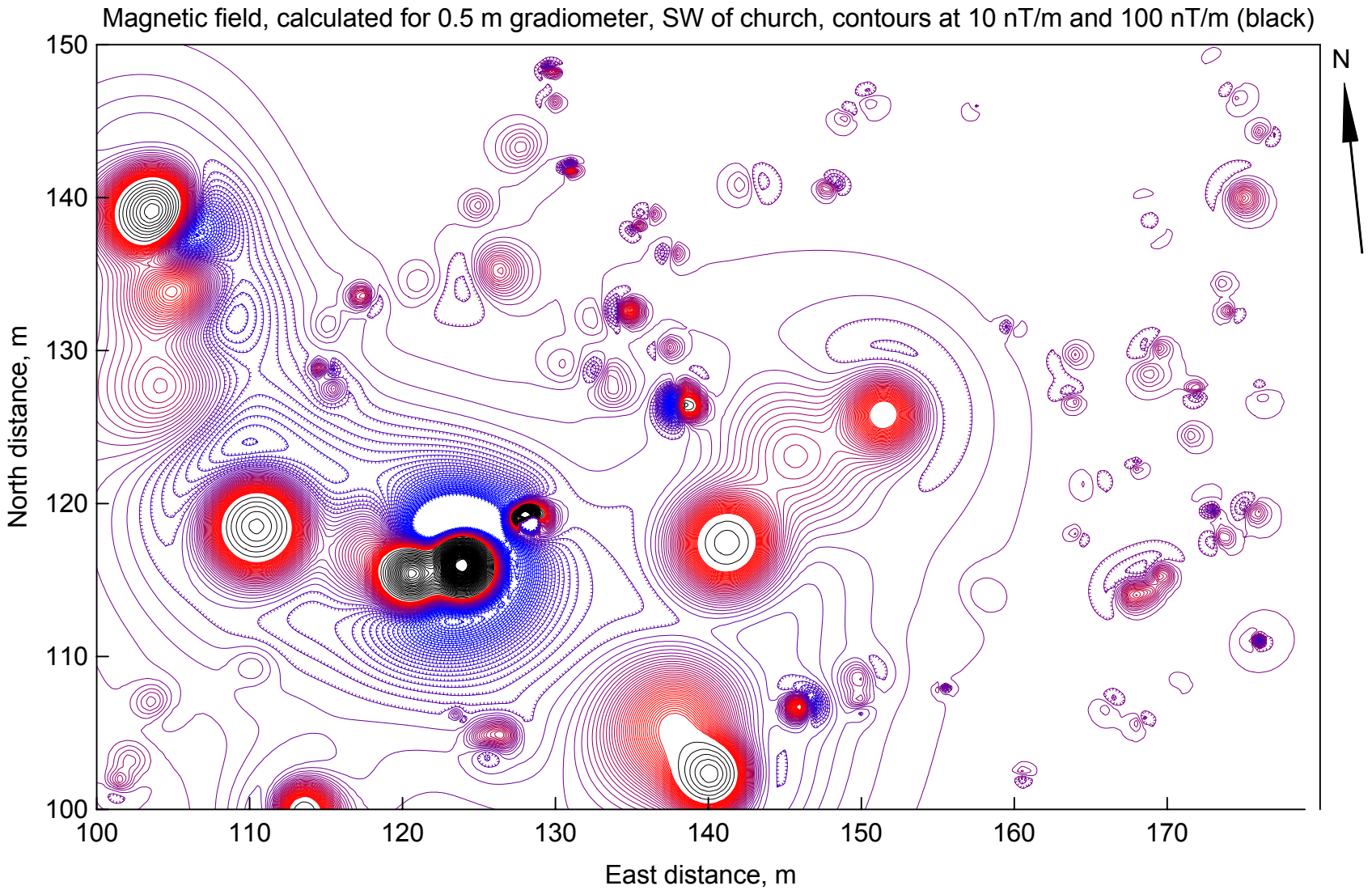

Figure 11: The effect of using a gradiometer. While Figure 9 displays a calculation of the total magnetic field, a calculation of the vertical gradient is shown here. The spacing between the magnetic sensors was assumed to be 0.5 m. Gradient measurements somewhat reduce the effect of the deeper geological features.

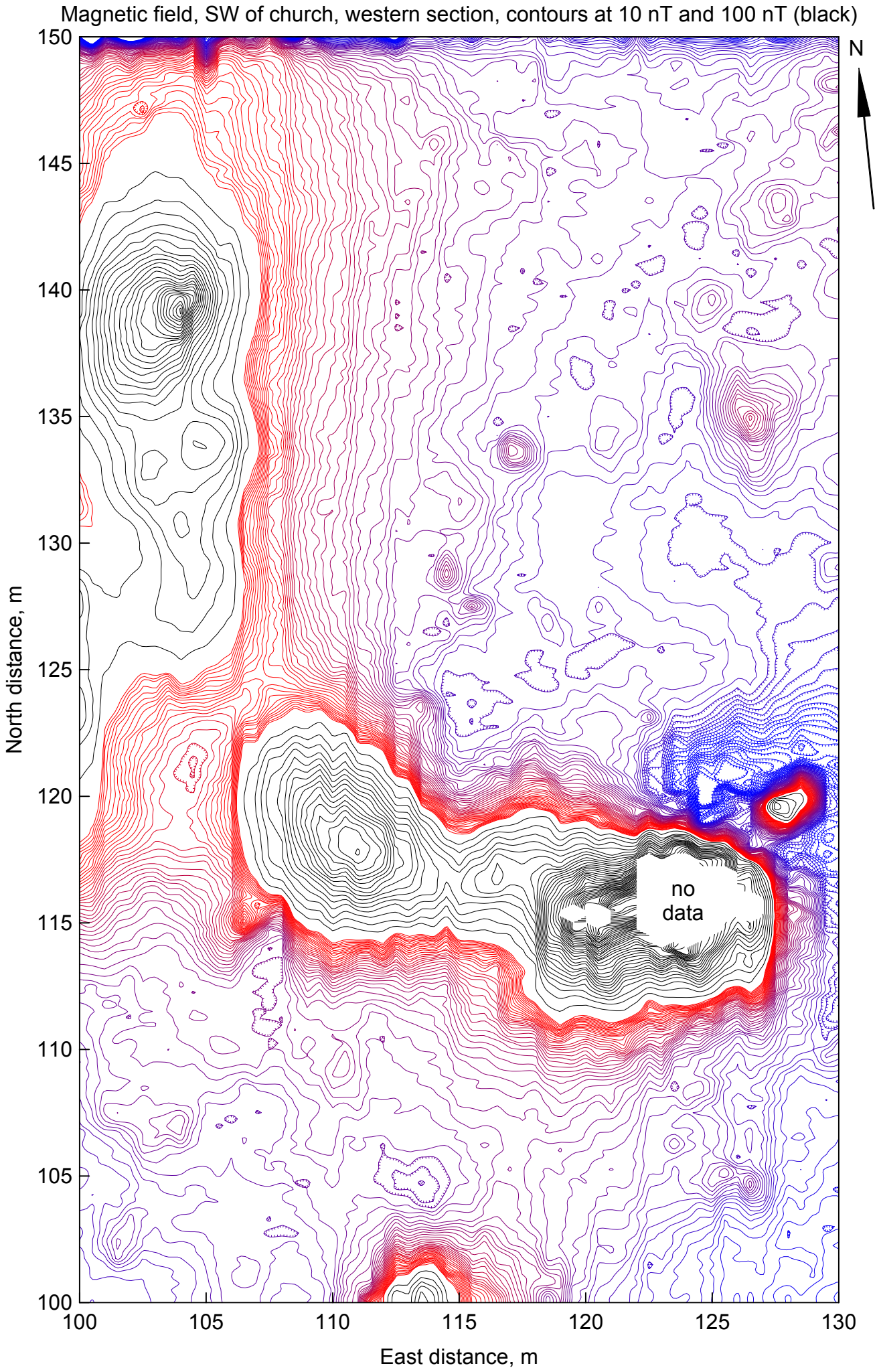

Figure 12: The western third of the magnetic map of the area SW of the church.

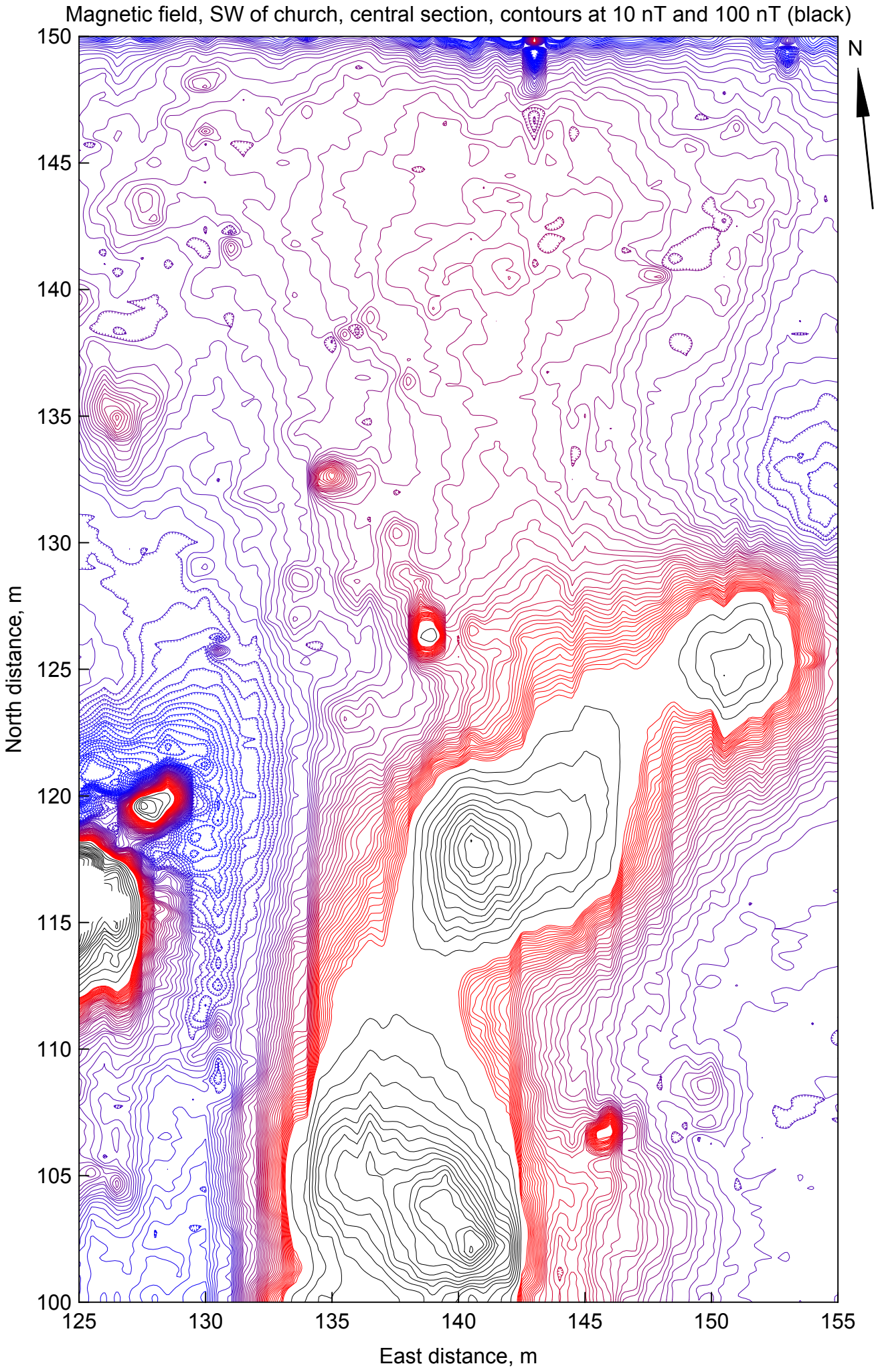

Figure 13: The central third of the magnetic map of the area SW of the church.

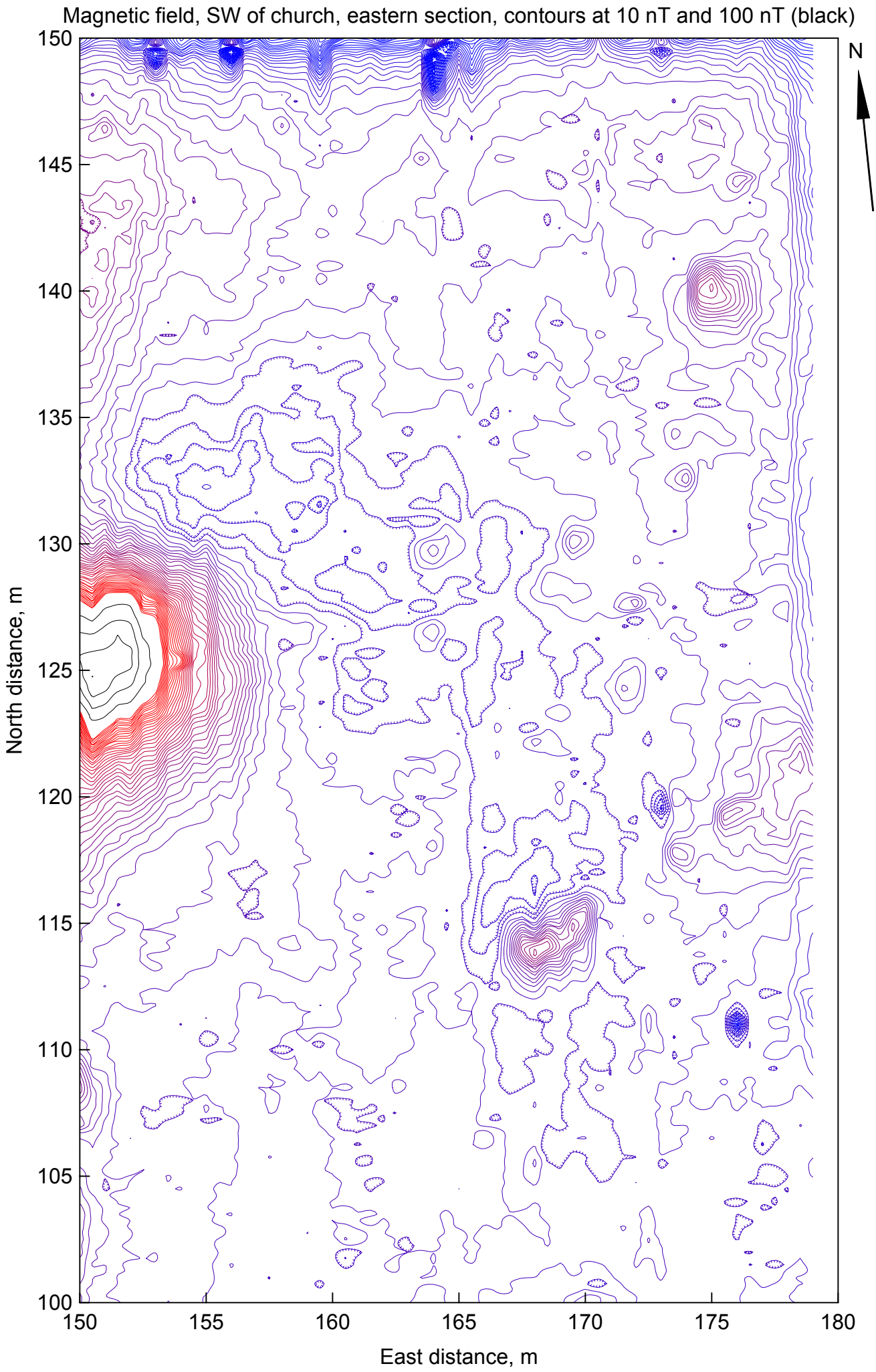

Figure 14: The eastern third of the magnetic map of the area SW of the church.

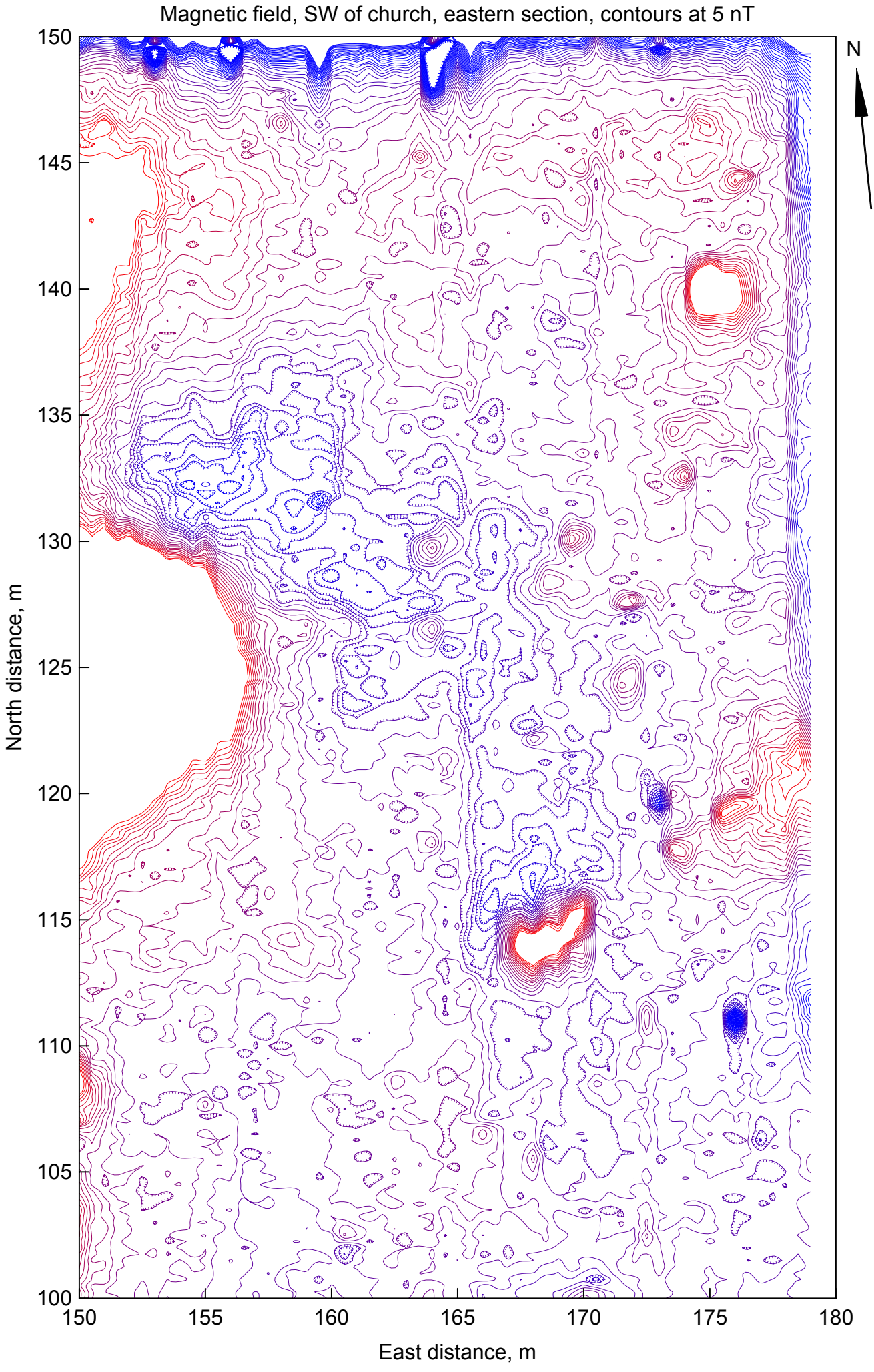

Figure 15: A redrawing of Figure 14 at a finer contour interval.

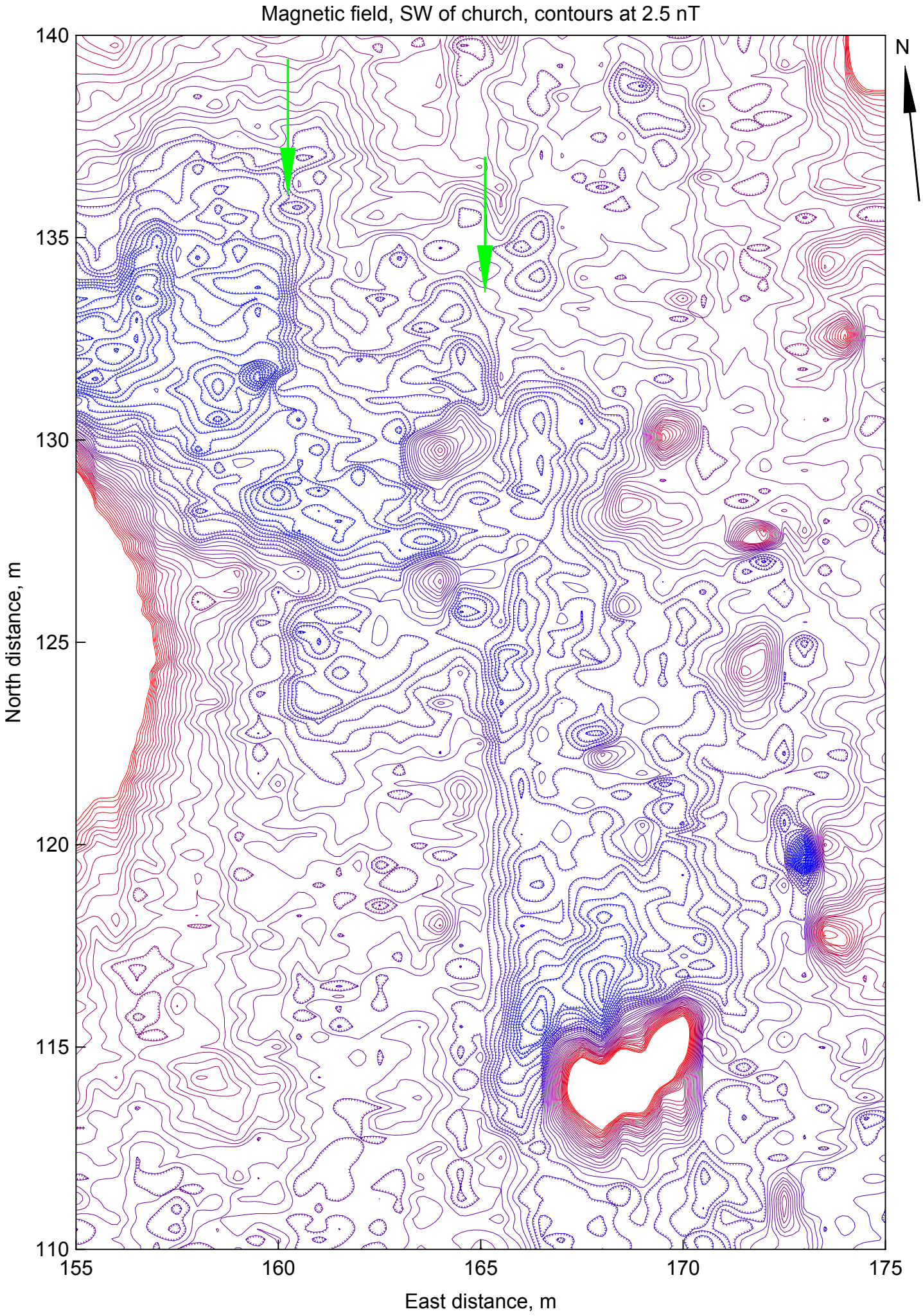

Figure 16: A further refinement of Figure 14, with a smaller area and contour interval.

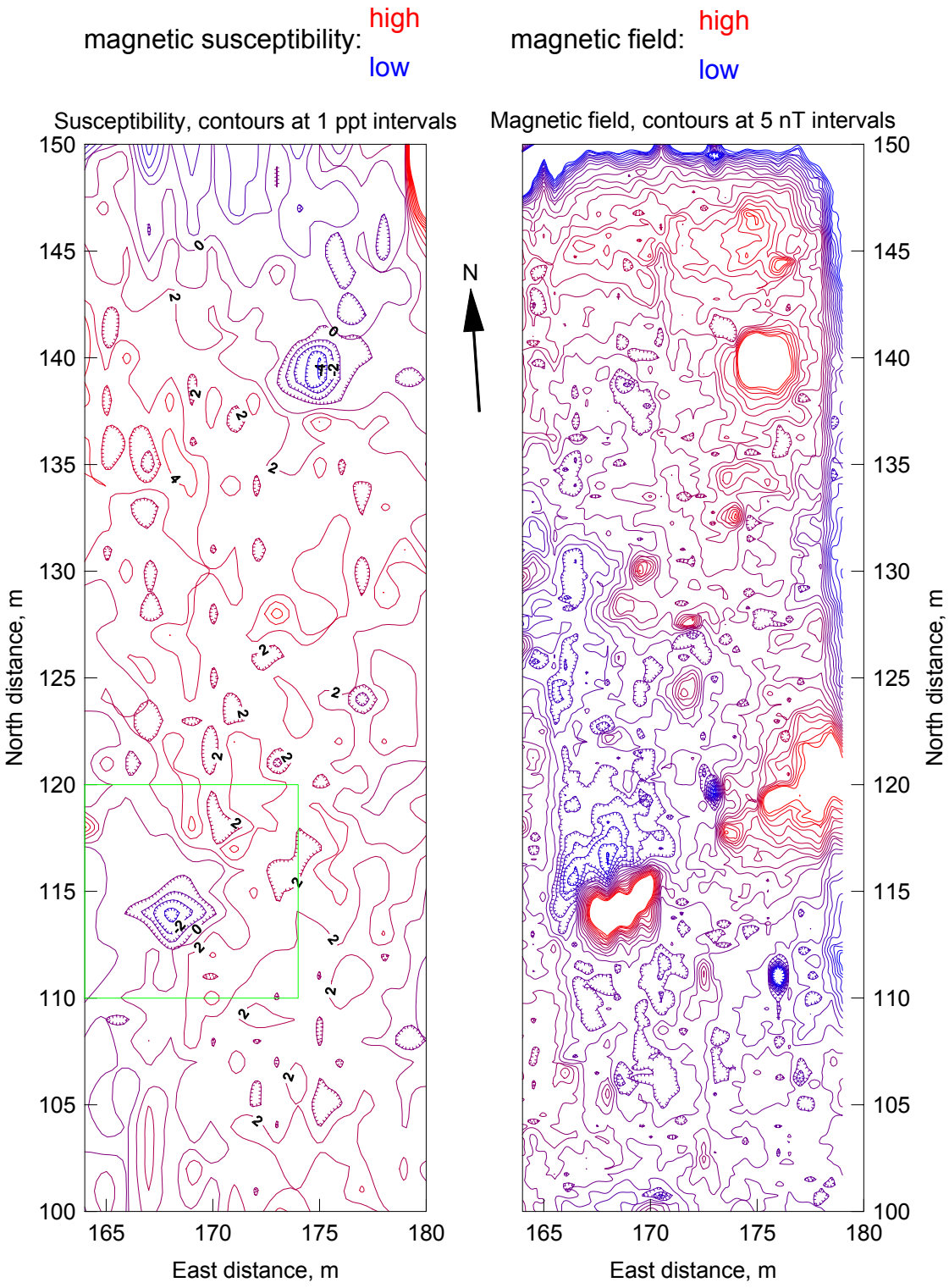

Figure 17: Two magnetic maps. A map of the total magnetic field is shown at the right, while a map of magnetic susceptibility of the same area is on the left. Both maps show the eastern end of the grid that was southwest of the church. The map of magnetic field is more detailed than the map of susceptibility. Two anomalies clearly match in the two maps: At E175 N140 and E168 N115. The susceptibility anomalies are lows; this is probably because magnetic features are deeper than 0.3 m underground. The green square locates the enlargement of Figure 23. The magnetic highs and lows are not fully-contoured; extreme readings are indicated as white areas inside dense contour lines.

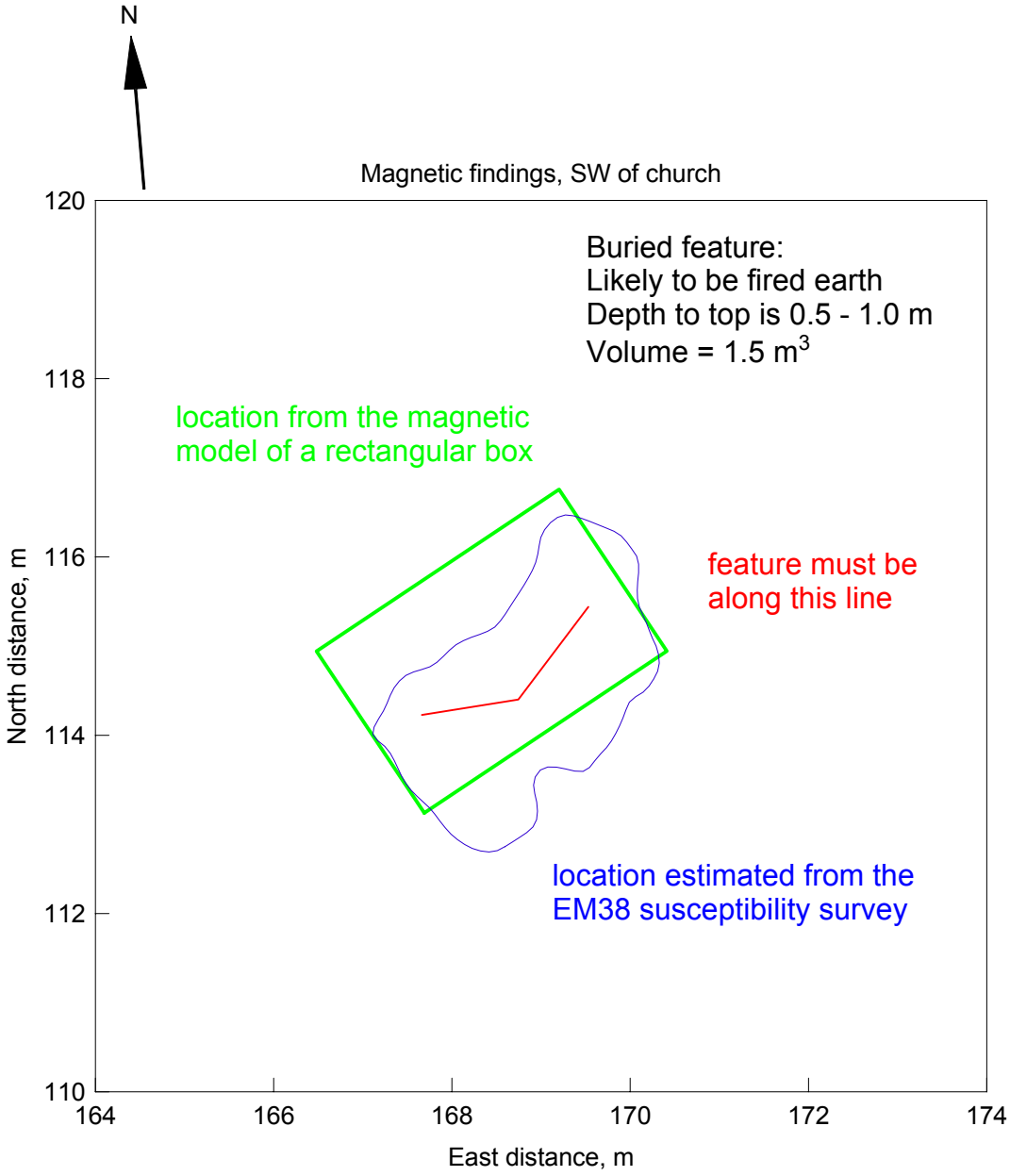

Figure 18: An interpretation of a major magnetic anomaly. This broad feature was detected clearly by both the magnetometer and the magnetic susceptibility meter. It is located most reliably at the overlap between the green and blue outlines; the red line marks the central span of the feature. The estimate of the volume of the feature is derived from the interpreted magnetic moment (3 Am^2) and typical parameters for fired earth (a relative magnetic moment of 1 mAm^2/kg and a density of 2 Mg/m^3). If the lateral dimensions of the feature are 3.3 by 1.4 m, then its thickness is estimated to be 0.3 m.

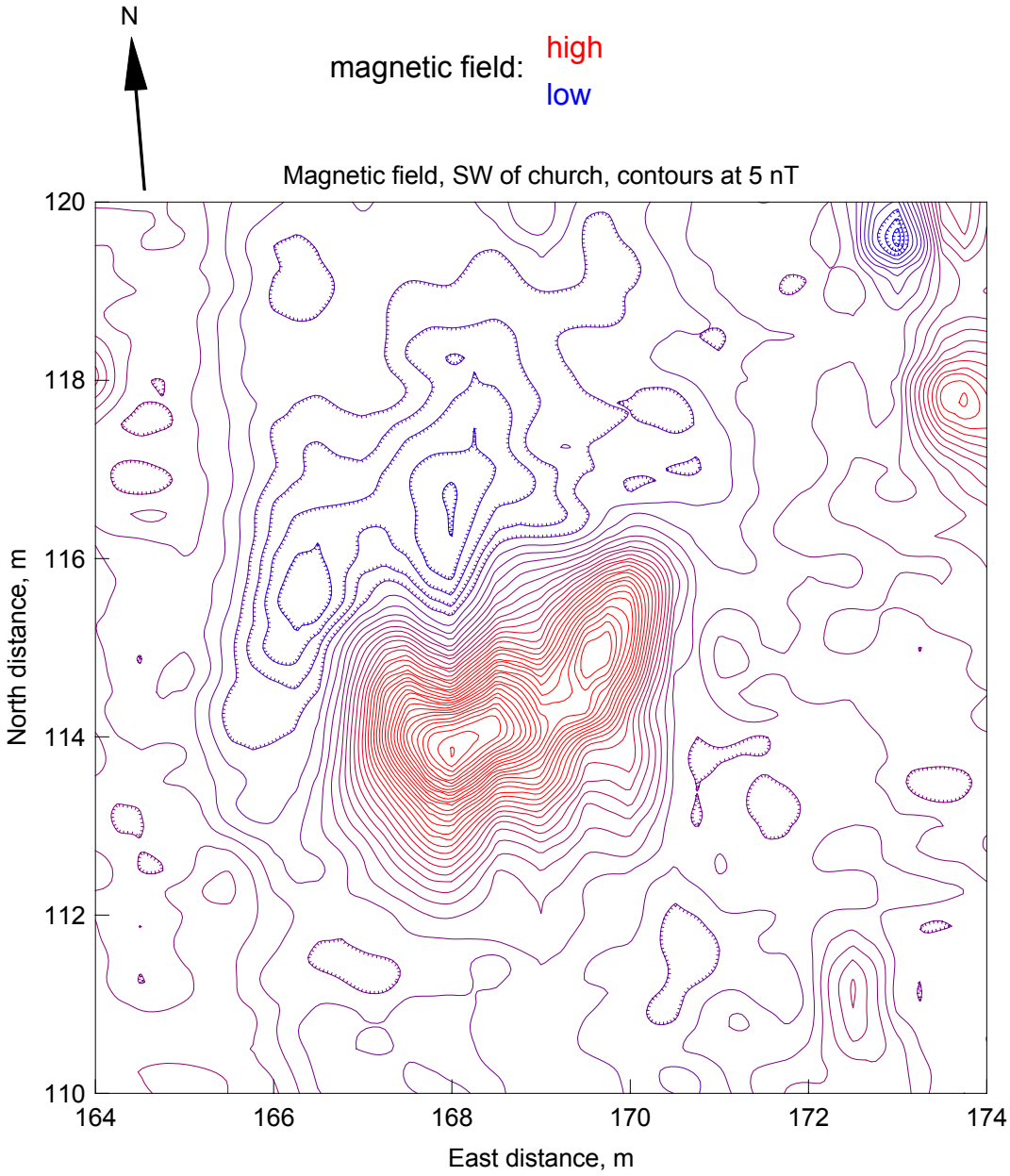

Figure 19: The magnetic map of the feature in Figure 18. This is just an extraction of the measurements from Figure 8. The height of the magnetic sensor was 0.3 m; readings were made at intervals of about 0.25 m along north-going traverses, and the spacing between lines of measurement was 0.5 m.

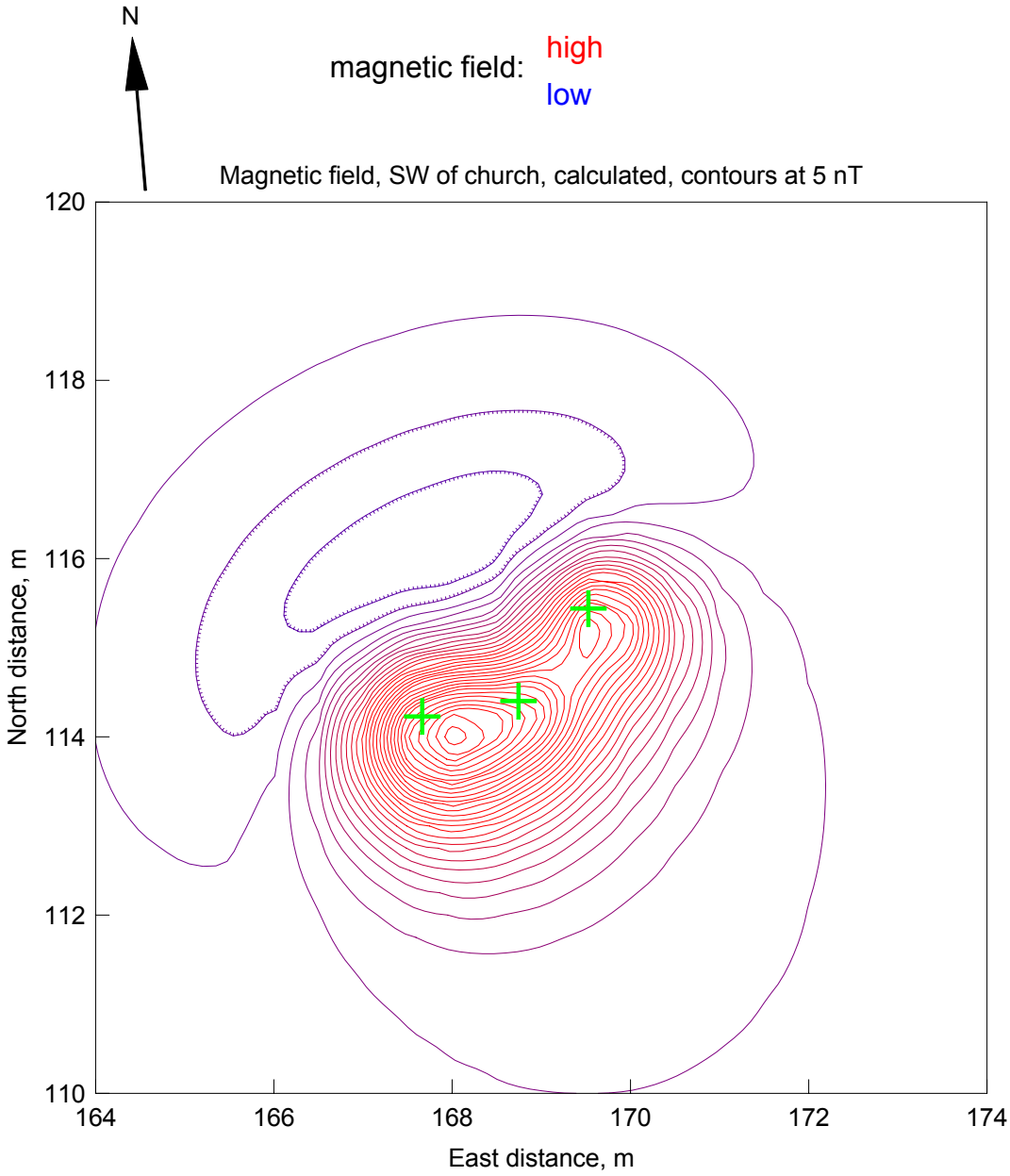

Figure 20: An approximation of the measurements in Figure 19 by three dipoles. The dipoles are located by green+ symbols; going from left to right, these are numbers 53, 42, then 47 (see Figure 39 for the parameters). The direction of magnetization of each dipole (I and D) was forced to remain the same as the other two; the resultant direction was I = 66°, D = -60°. The total magnetic moment of these three dipoles is 4.5 Am^2, and their depths were (left to right): 1.26 m, 0.89 m, and 0.98 m. While the calculations provide a good match to the measurements, the dipoles may be a little too deep.

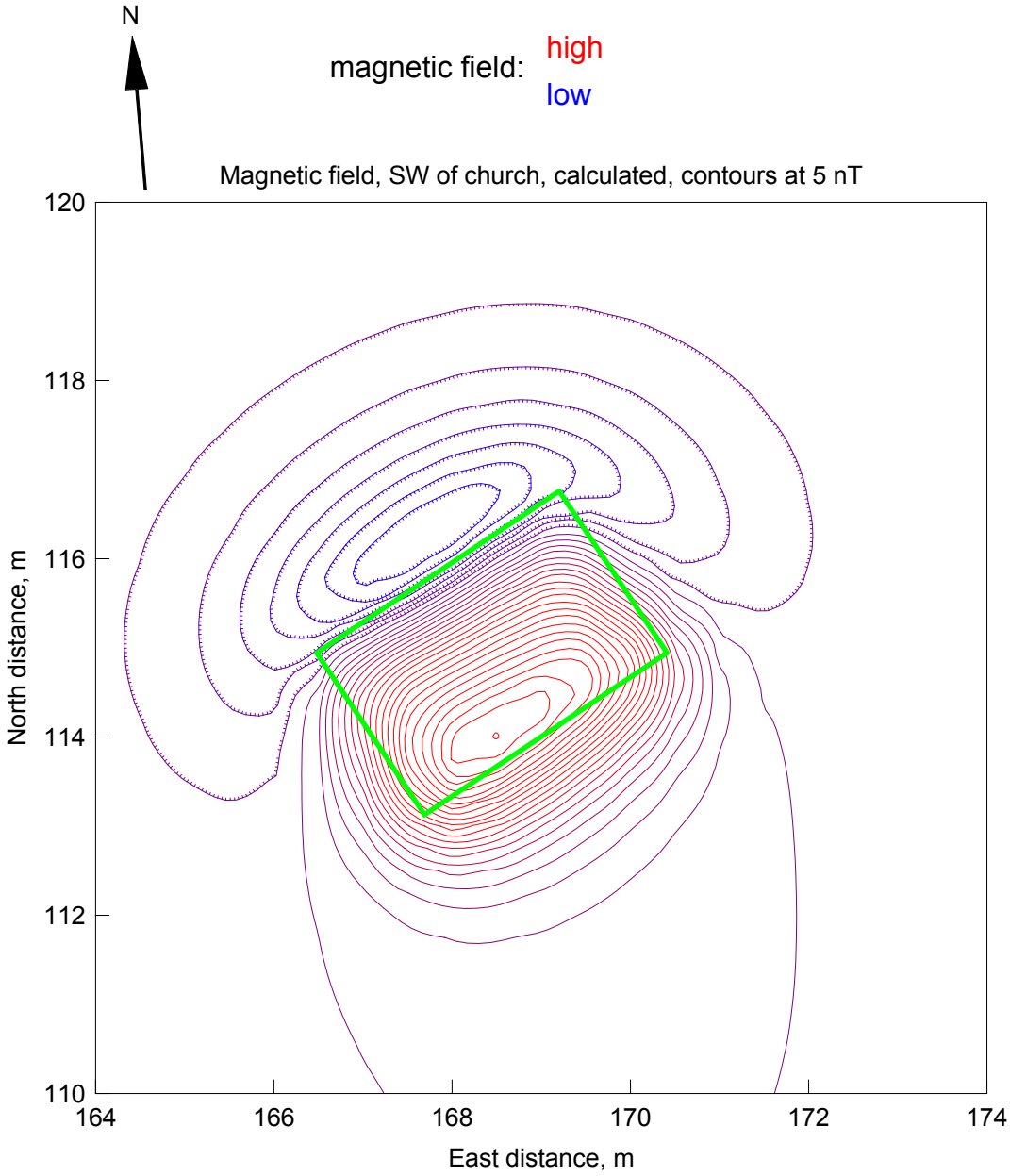

Figure 21: Another magnetic model of the measurements in Figure 19. The rectangular body is outlined in green. The total magnetic moment of this body was 3.2 Am^2, and the depth to its middle was 0.6 m. The direction of total magnetization within the magnetic box was: I = 51°, D = -24°. This simple magnetic model also provides a good approximation of the measurements.

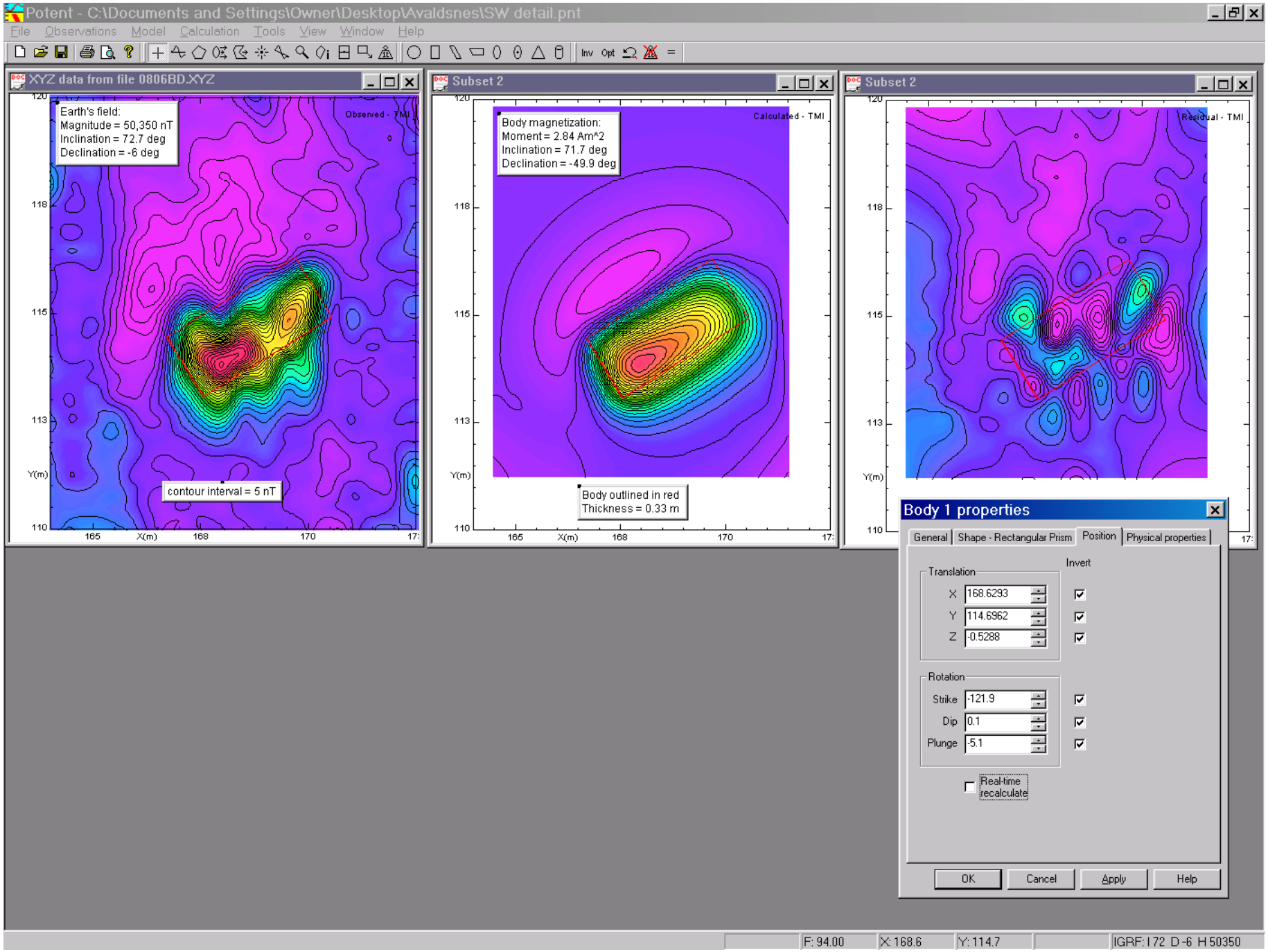

Figure 22: Another model with a magnetic box. This analysis was done with the program Potent, and it allows the box to be tilted (note the Plunge of 5.1° at the lower right). Left to right, the maps along the top are: Measurements, calculations, residual.

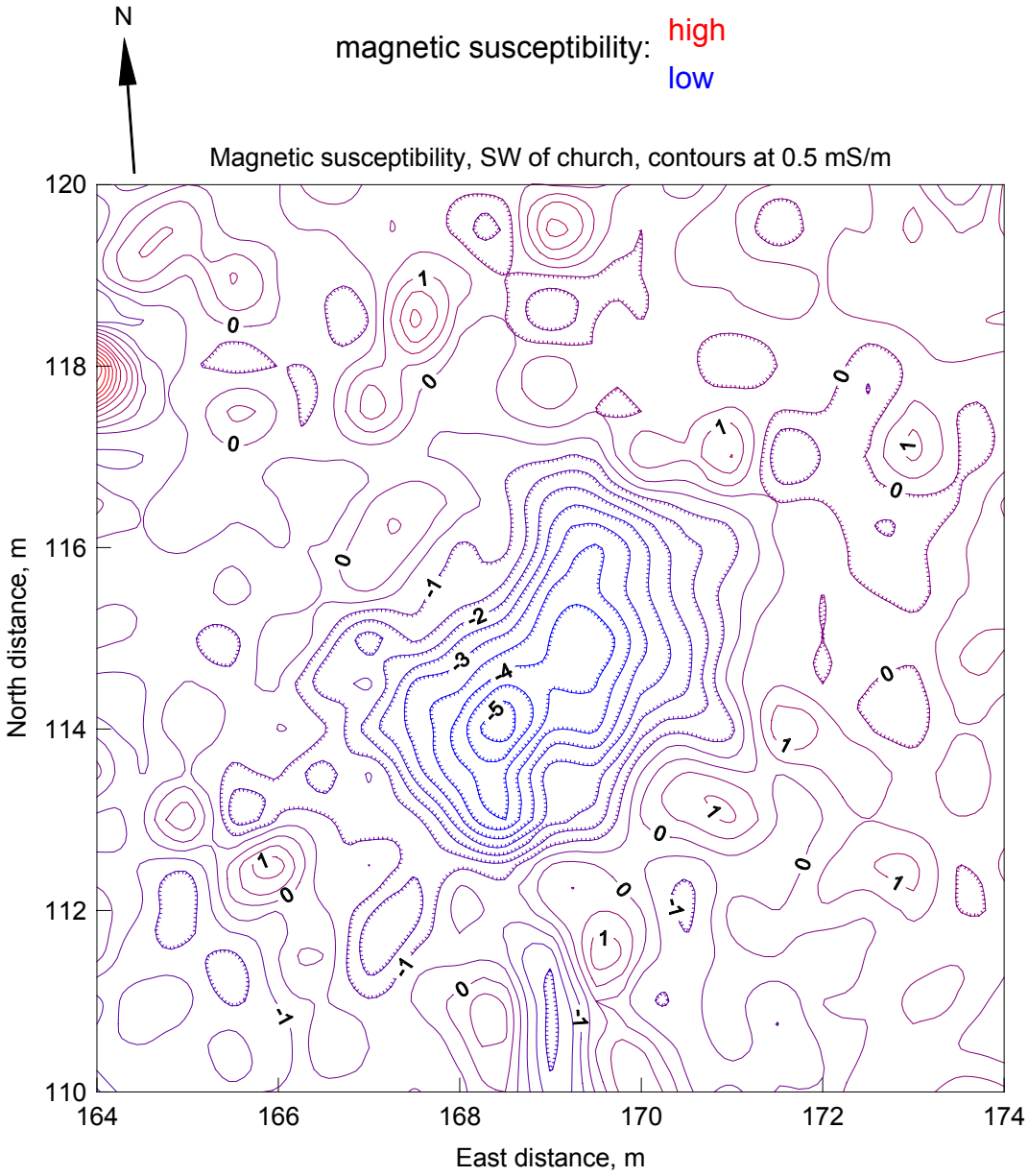

Figure 23: Magnetic susceptibility in the area of Figure 18. The central anomaly is primarily a low; this is because the main part of the magnetic feature is below a depth of 0.3 m (see Figure 40). This survey was done with Dagfinn Skre. The measurements with the EM38 were made at intervals of 0.5 m in both directions. The magnetic dipoles of the EM38 were vertical and the bar was extended north-south; the instrument was held at a height of 0.3 m.

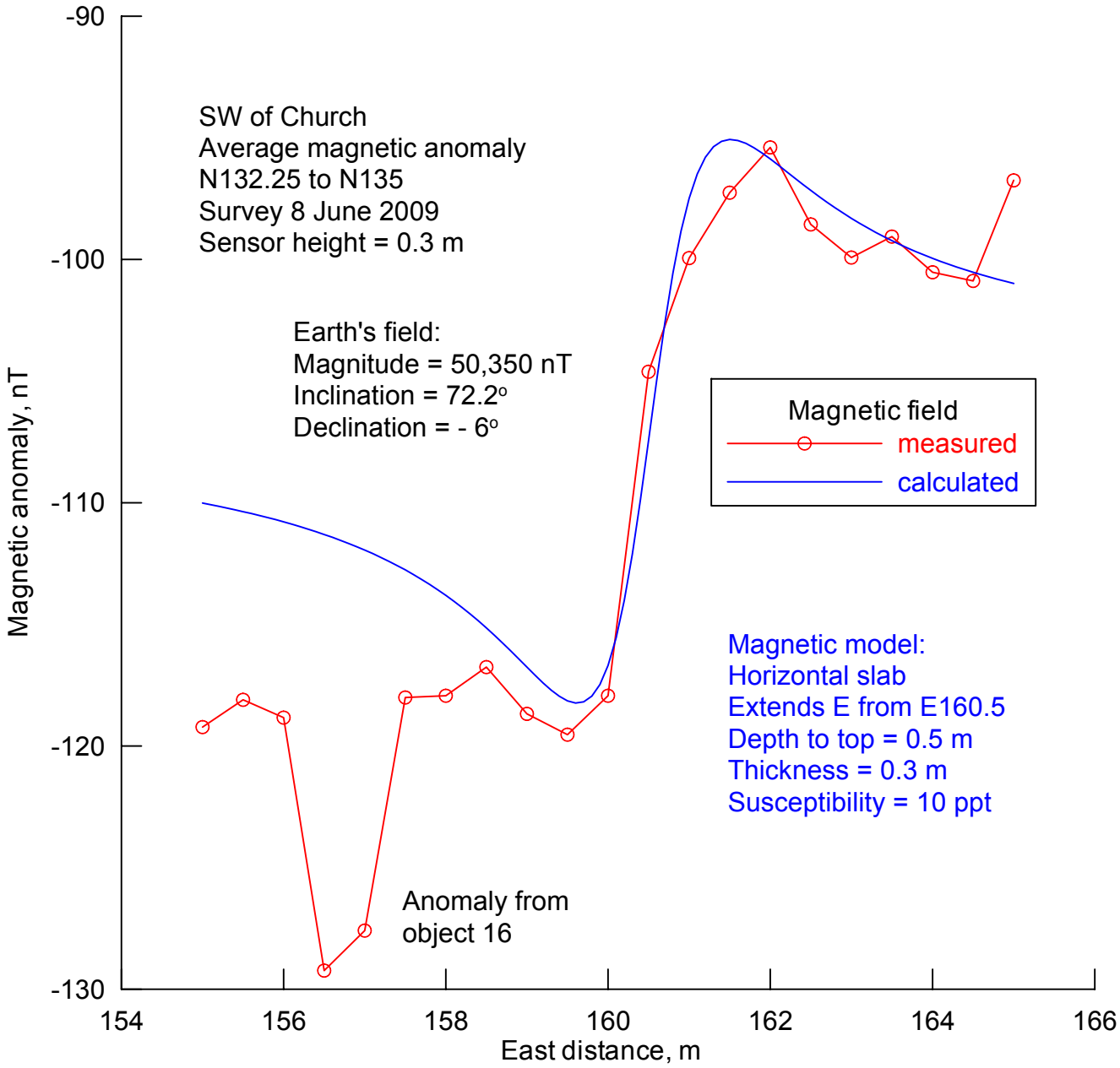

Figure 24: An explanation for some linear anomalies in the magnetic map. The interpretation in Figure 5 locates several abrupt magnetic boundaries. The averaged readings across one of these features are plotted with a red line. The calculated field of the blue line is a good approximation to the measurements. This analysis suggests that a magnetic slab extends to the east from E160.5 at a depth of 0.5 m. At the other four magnetic boundaries in Figure 5, the magnetic slab extends to the west.

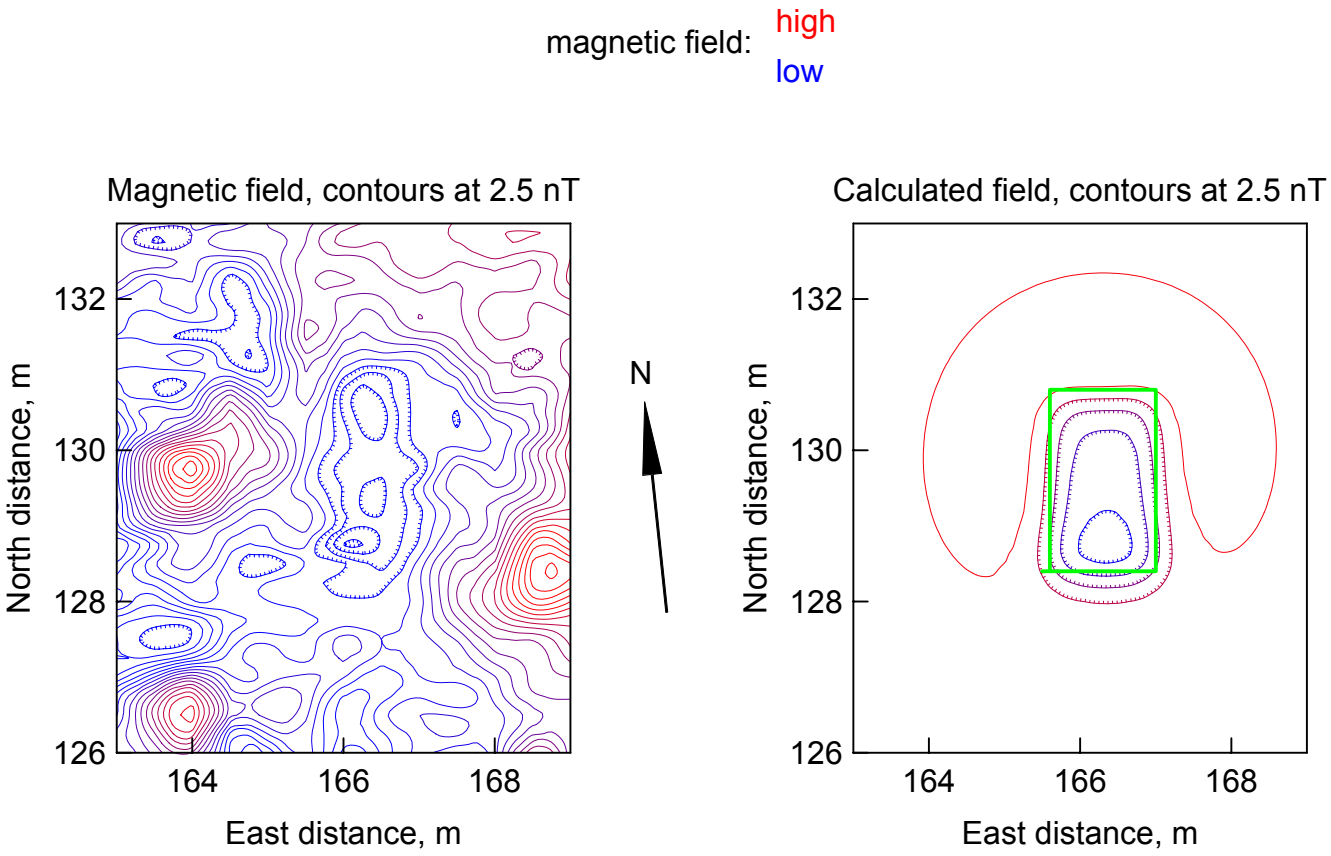

Figure 25: A possible explanation for some elongated magnetic lows. Four of these are located in Figure 5 as rectangles that are marked with black, dashed lines. The magnetic map of the southern-most of those is enlarged on the left. The calculations on the right approximate the magnetic anomaly. This model body is a rectangular box (green) and it extends between a depth of 0.1 and 0.4 m. The magnetic susceptibility of the soil in the box was assumed to be 2 ppt below that of the surrounding soil. This model suggests that the normally-magnetic topsoil at this location has been replaced by rather non-magnetic soil (this replacement soil may be contain a greater fraction of quartz sand).

Figure 26: A photograph of the survey area northeast of the church. The tape measure is along line N100 and the nearby flagged stake is at coordinate E130 N100. The view is uphill to the west. The stone wall in the background splits the area into two sections. The historic church is on the left. Note the tall monolith there; it is not quite touching the wall of the church (and that is important).

Figure 27: Another view of the northeastern area. Mainland Norway is in the background. The two ships that are docked near the shore probably cause a significant anomaly at Tatiana's magnetometer (perhaps about -10 nT). However, because the lateral gradient of that anomaly is very low, they did not interfere with the magnetic survey. This photo was taken by Marit Synnøve Vea.

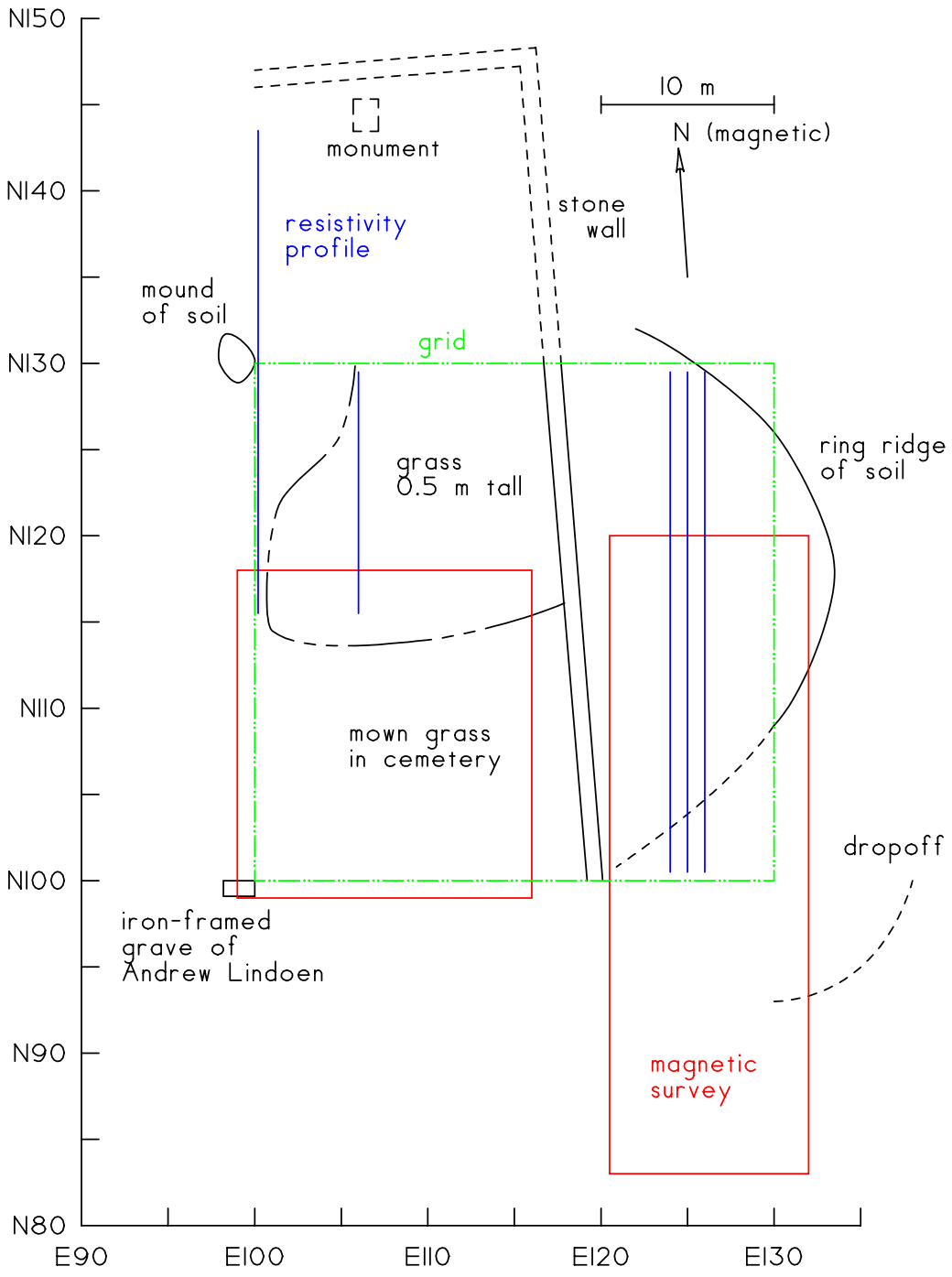

Figure 28: The area of survey in the northeast. A square grid, 30 m on a side, was set up with assistance from Dagfinn. The geophysical measurements extended outside that square. In this area, a resistivity survey substituted for the EM38 susceptibility survey that was done to the southwest. This area can be relocated from the grave at its southwest corner; the grid was aligned with the length of that grave. The at-surface features that are marked with dashed lines have locations that are approximated.

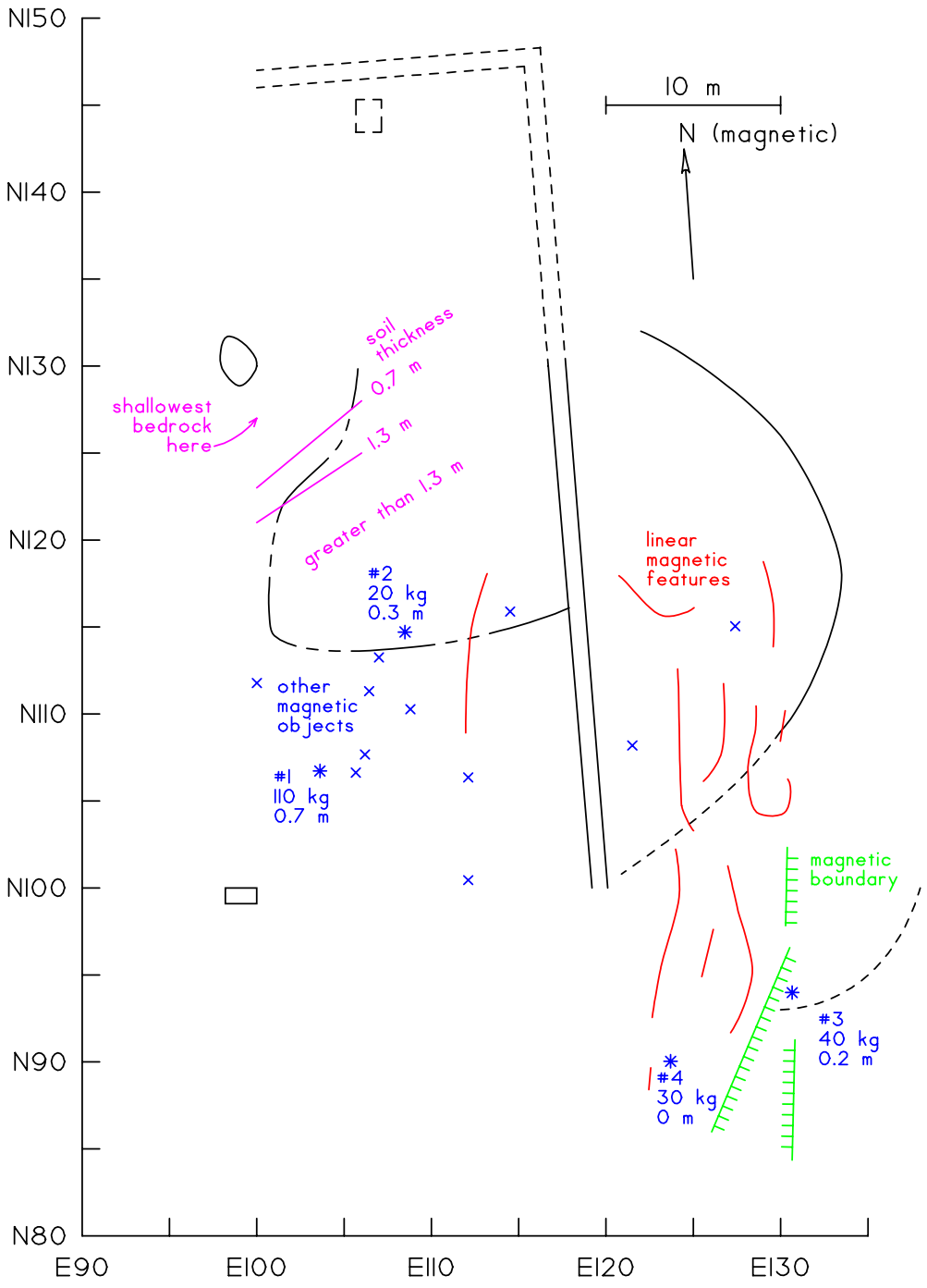

Figure 29: Findings in the northeastern area. There was an unusually large difference in the patterns on the two sides of the stone wall. To the east of the wall, linear features that were very magnetic were revealed, and the soil appears to be uniformly deep. On the west side of the stone wall, magnetic features are relatively rare, and bedrock approaches the surface in the northern part of the area of survey.

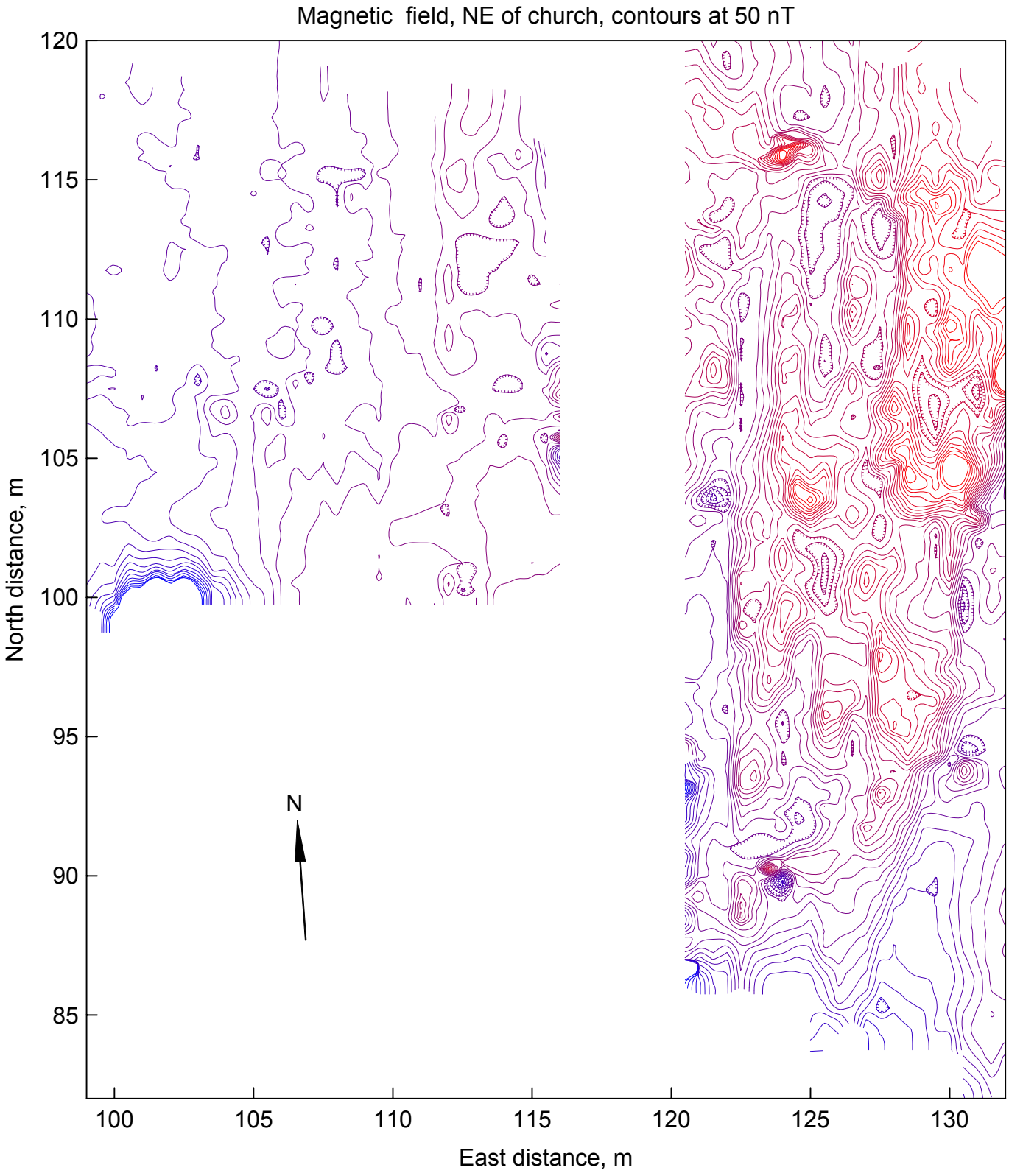

Figure 30: A magnetic map of the northeastern area. The contour lines have been drawn to clarify the strong anomalies on the eastern side of the stone wall (the blank area between the two sections). Magnetic highs are red, while lows are blue. Note that the anomalies to the west are quite weak.

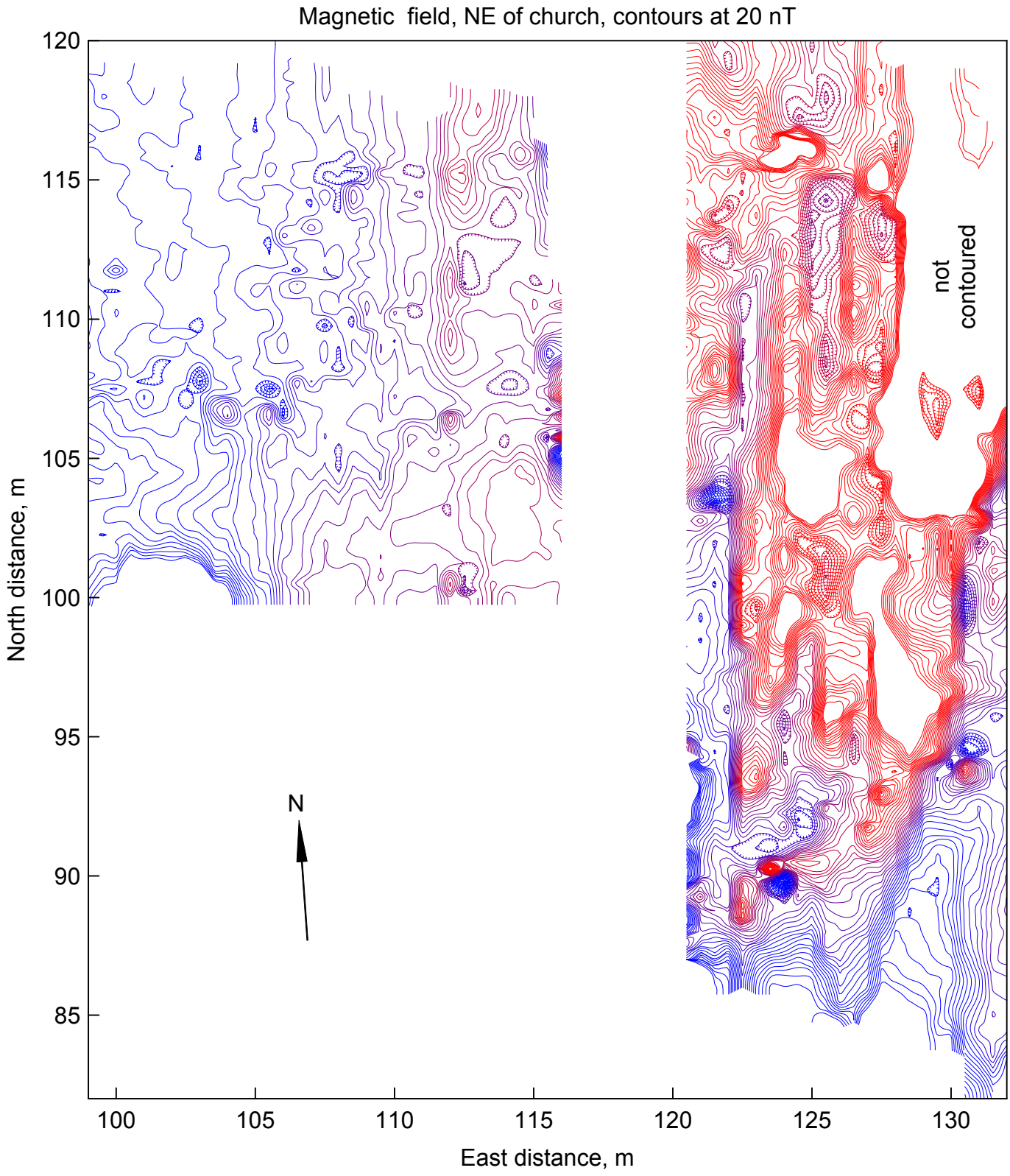

Figure 31: A redrawing of Figure 30. With a closer interval between contour lines, the anomalies in the western section are clearer, while those on the east are not contoured completely. In the western section, some small-area anomalies are now evident.

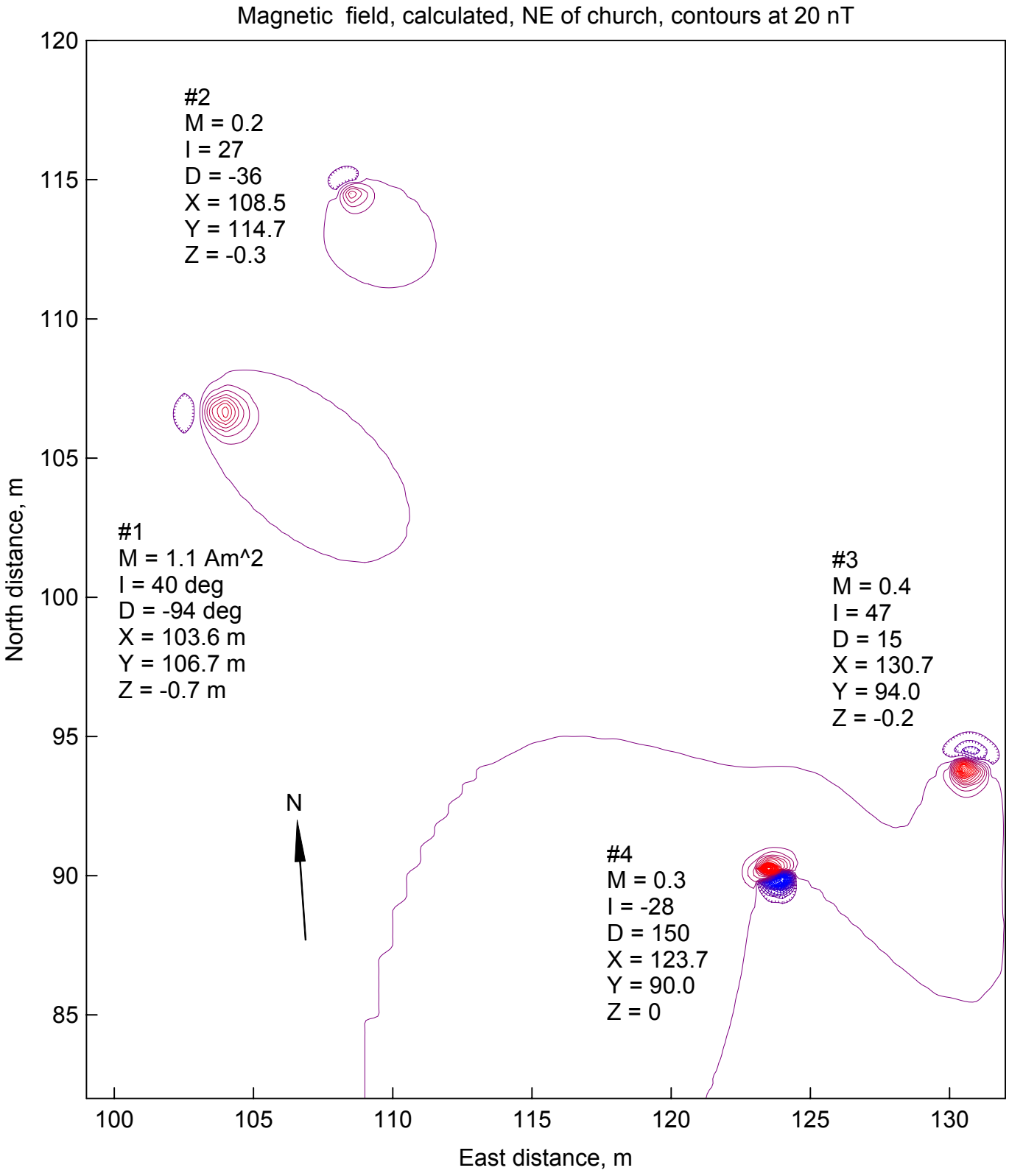

Figure 32: An analysis of four magnetic anomalies. The magnetic field was calculated from the dipolar parameters that are listed here. Since the patterns of this calculation are similar to the measurements in Figure 31, the parameters may be good approximations of those of the underground bodies. Their depths range between 0 and 0.7 m.

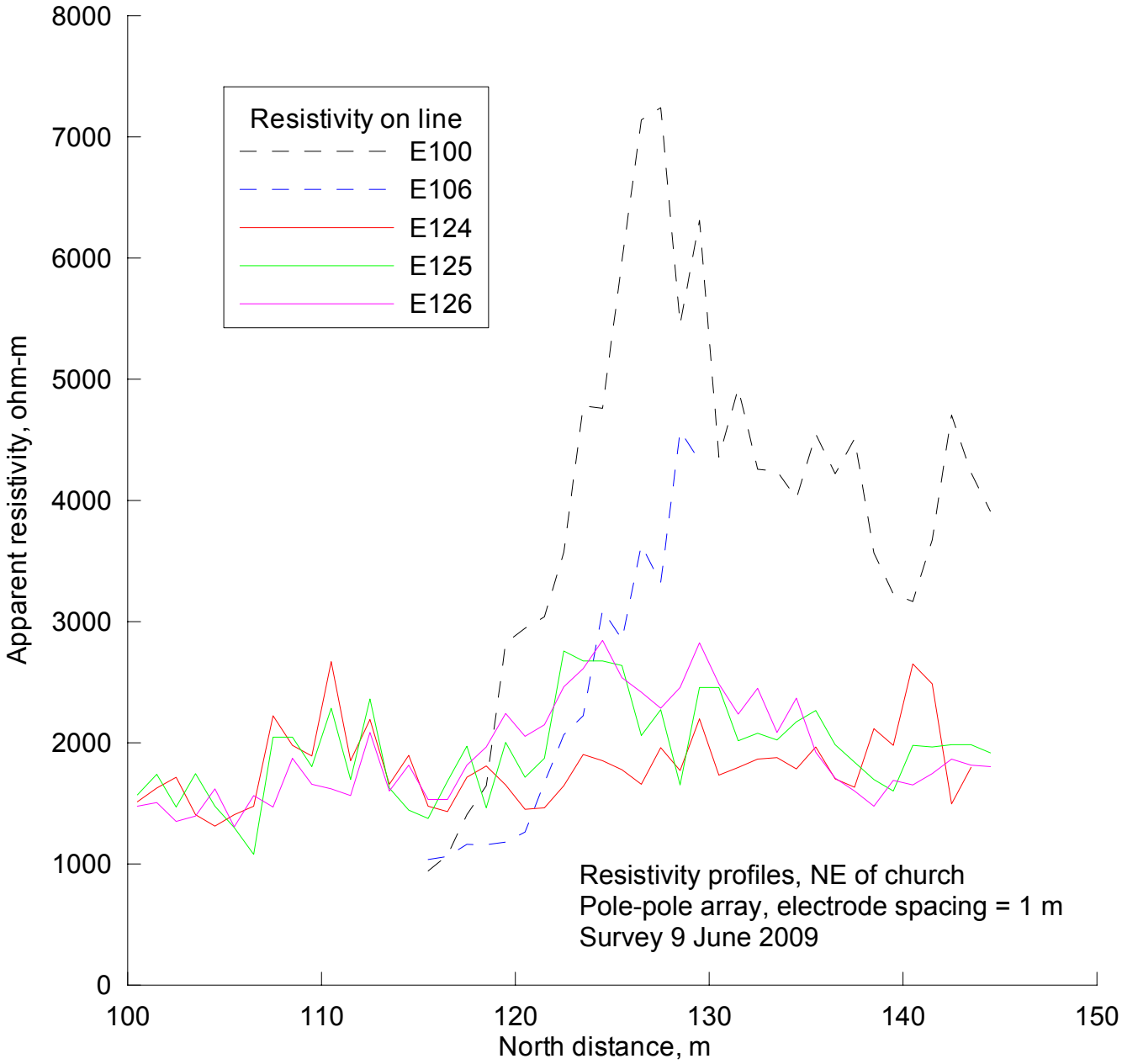

Figure 33: Resistivity measurements in the area northeast of the church. West of the stone wall (lines E100 and E106), the resistivity rises to high values going north. The high readings are probably caused by shallow bedrock, and it may be within 0.1 m of the surface near E100 N128, where the peak reading of resistivity is found. East of the wall, the readings remained at rather low and constant values.

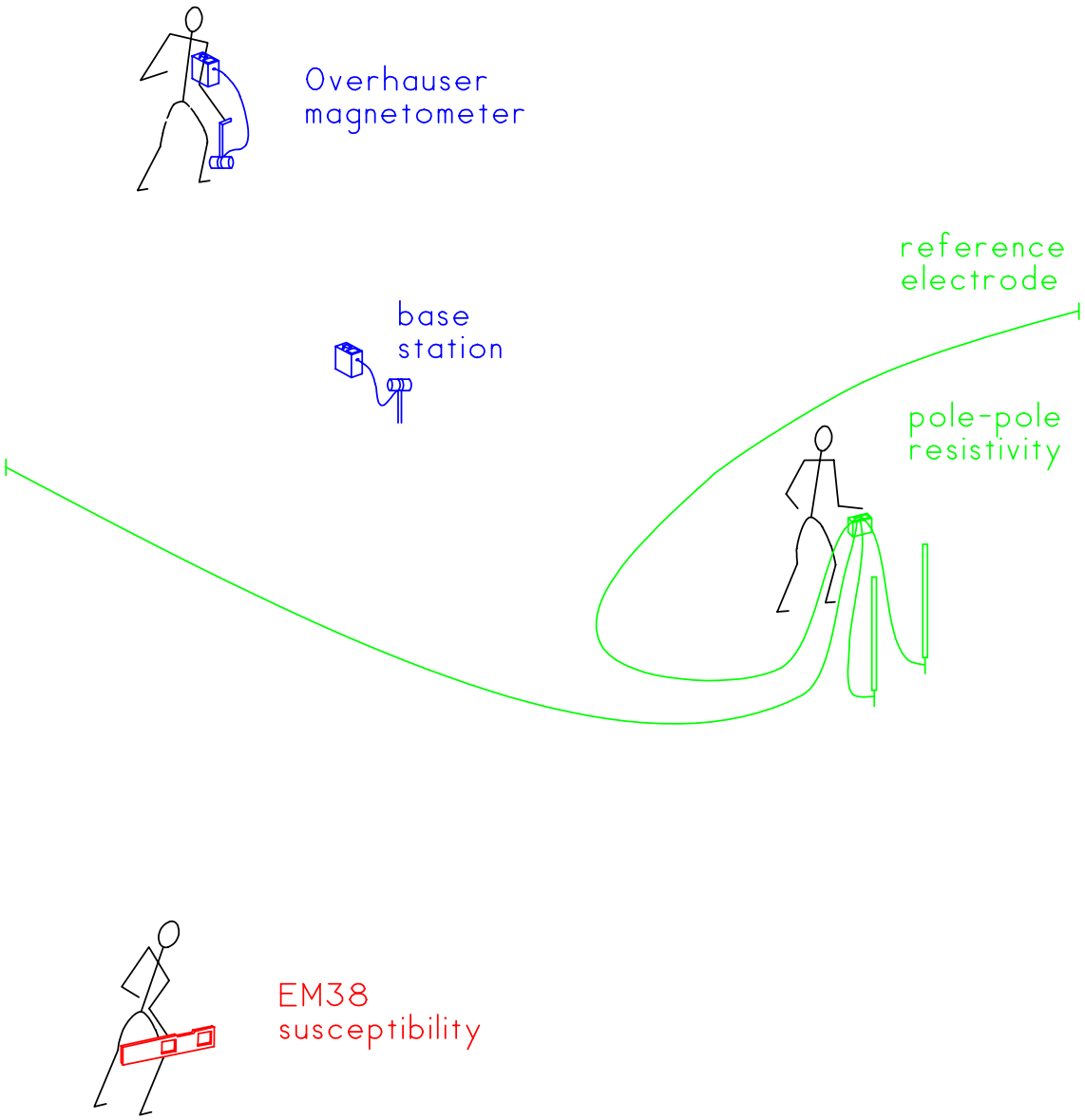

Figure 34: The geophysical instruments. The largest areas were explored with a magnetometer. This was a model GSM-19WG Overhauser instrument that was manufactured by Gem Systems. Two almost-identical instruments were applied to this survey. One had its sensor carried around the areas of survey at a height of 0.3 m above the soil; the other instrument remained stationary and recorded the natural changes in the Earth's magnetic field.

The model EM38 electromagnetic induction meter was tested only in the area southwest of the church. This instrument was operated in its magnetic susceptibility mode, and it was carried at a height of 0.3 m above the soil's surface with the aid of a shoulder strap, not shown in this drawing.

Resistivity profiles were measured in the area northeast of the church using a model 4610 meter manufactured by AEMC. The pole-pole configuration of electrodes was applied to the survey; two of the electrodes remained fixed at distant points for the entire survey.

Figure 35: The Gem Systems magnetometer. Tatiana is carrying the magnetic sensor (white cylinder) with her right hand, while she presses a button on the display console to mark intervals of 1 m along the guide rope (note the blue flags). In the background, Bruce (on the left) and Dagfinn have halted their susceptibility survey in the southwestern area in order to allow the faster magnetic survey to pass by. This photograph was kindly supplied by Marit Synnøve Vea. The view is to the southwest.

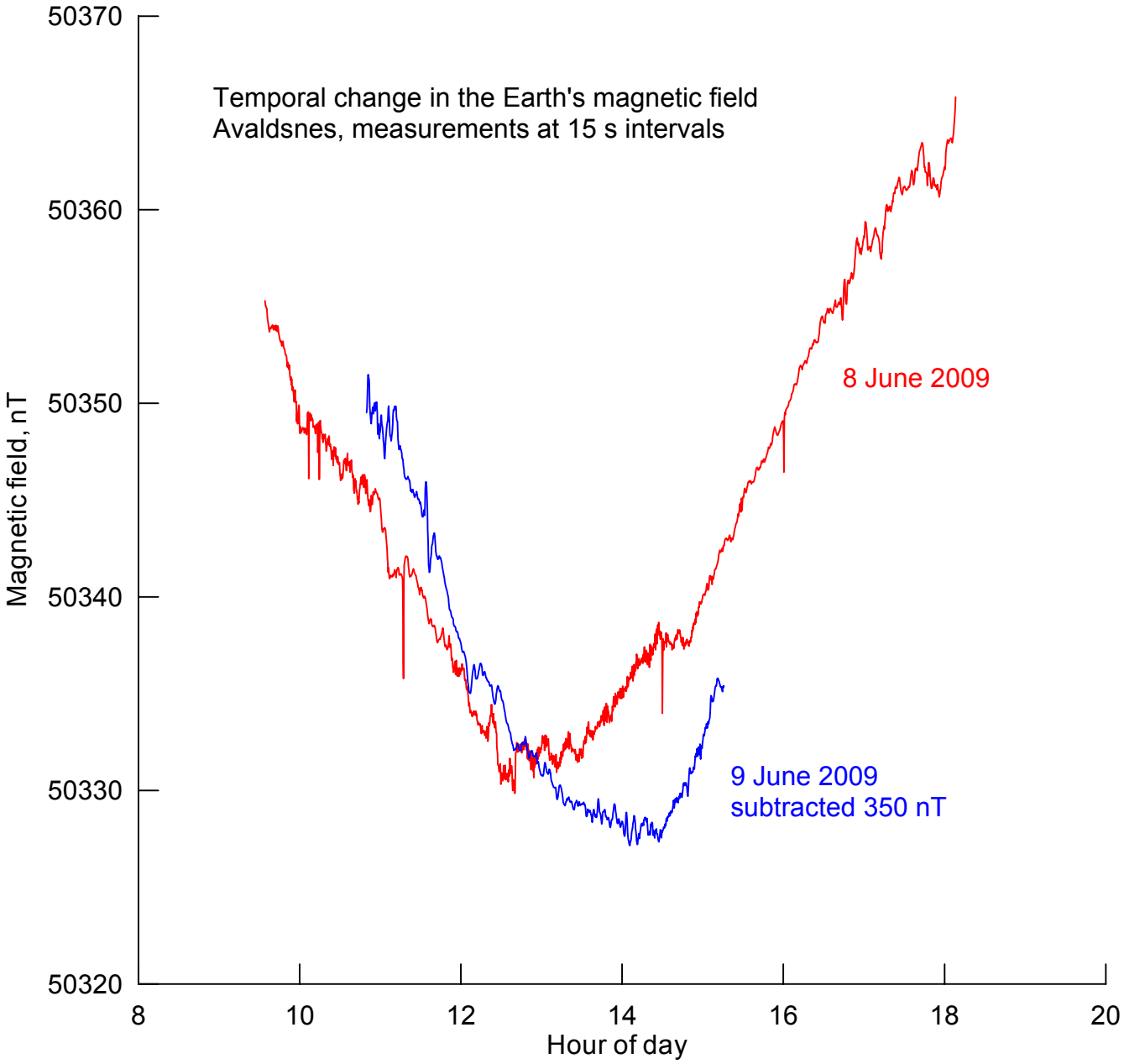

Figure 36: Diurnal changes in the Earth's magnetic field. These recordings were measured on the two days of field work. The usual dip in the field near local noon is evident on both days. On June 8, the five abrupt downward spikes (2 - 5 nT) in the magnetic field are caused by passing trucks or by a person near the magnetic sensor of the base station magnetometer.

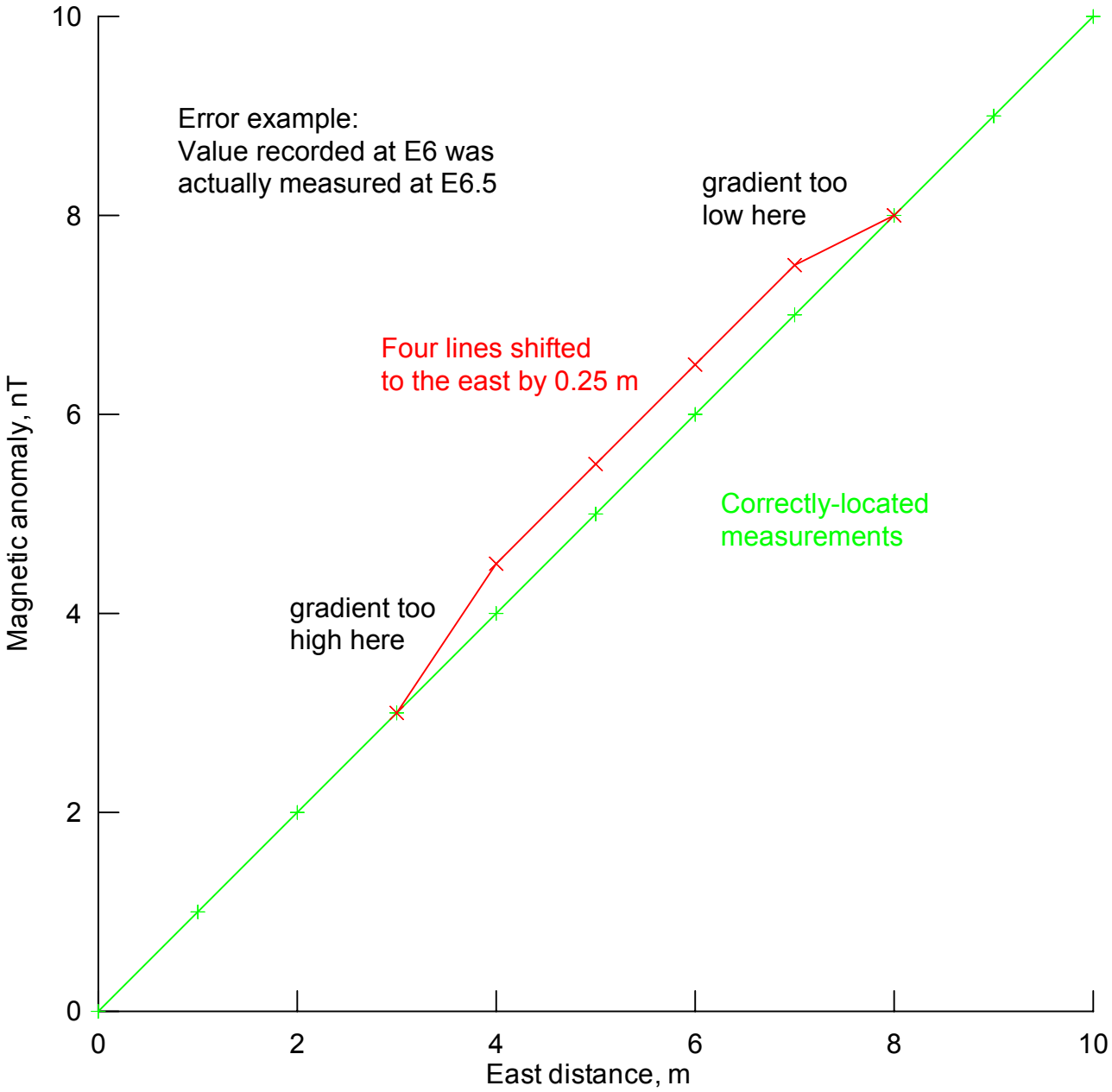

Figure 37: The effect of a shift in the location of a traversing cord. In the southwestern area, the tall grass made it difficult to place the traversing cord at the correct location. During the magnetic survey of that area, four traverses were made for every time the cord was moved. If the cord was set at an incorrect location, the resulting magnetic patterns could show a narrow band with an abnormally high lateral gradient on one side, and another band with a low gradient on the other side of the group of four lines.

#	M Am^2	I deg	D deg	X m	Y m	Z m
1	0.009	-18.00	65.43	155.36	107.93	0.00
2	0.051	44.00	-53.00	129.66	148.34	0.00
3	0.065	12.00	-46.00	131.00	141.97	0.00
4	0.010	4.45	77.14	157.47	145.78	-0.02
5	5.773	-33.46	147.63	128.21	119.05	-0.04
6	0.020	2.47	-42.66	167.98	122.49	-0.14
7	0.086	-47.14	81.51	175.76	111.08	-0.17
8	0.049	17.84	-124.32	135.25	138.15	-0.18
9	0.067	15.88	170.84	171.82	127.42	-0.25
10	0.037	26.38	144.41	123.62	106.12	-0.26
11	0.038	-5.72	185.46	160.62	102.26	-0.27
12	0.081	13.66	-90.36	136.13	138.99	-0.33
13	0.067	43.84	-76.54	129.74	146.36	-0.35
14	0.096	-42.08	-52.64	173.00	119.50	-0.36
15	0.027	8.69	-127.48	170.48	108.16	-0.38
16	0.066	-16.50	-74.42	159.81	131.57	-0.38
17	0.047	22.73	120.50	164.07	117.97	-0.39
18	0.171	13.90	55.86	147.98	140.83	-0.39
19	0.098	27.05	108.20	174.14	132.58	-0.40
20	0.236	26.47	103.85	114.85	128.84	-0.41
21	0.078	3.95	65.94	168.31	105.81	-0.44
22	0.116	22.63	111.50	176.37	144.30	-0.44
23	0.178	5.86	-85.67	137.57	136.45	-0.46
24	0.097	13.91	39.42	149.00	145.50	-0.50
25	0.134	23.98	-21.50	163.70	126.95	-0.51
26	0.255	20.72	-106.85	173.43	117.77	-0.59
27	0.088	8.06	-13.45	176.15	127.40	-0.61
28	0.224	15.63	167.73	149.87	106.92	-0.61
29	0.847	1.34	-121.67	138.14	127.35	-0.62
30	0.147	11.89	-57.69	174.34	146.83	-0.65
31	0.109	65.34	272.78	173.53	134.47	-0.66
32	0.149	-0.45	-15.32	150.43	146.69	-0.67
33	0.299	38.08	-63.56	169.33	130.33	-0.70
34	0.157	-1.25	36.55	166.23	107.01	-0.70
35	0.447	19.20	-64.86	175.51	119.62	-0.71
36	1.527	29.44	-92.50	134.54	132.66	-0.73
37	4.098	26.77	-101.07	138.33	126.44	-0.76
38	2.623	36.22	76.53	146.10	106.84	-0.77
39	0.853	45.98	114.60	117.48	133.57	-0.79
40	0.477	45.48	-98.20	137.27	130.26	-0.81
41	0.350	44.18	-115.27	163.74	129.71	-0.87

Figure 38: Magnetic parameters for objects in the southwestern area. The dipole numbers (on the left) match those in Figure 7. Red numbers indicate those dipoles whose parameters have a low accuracy. The Z parameter is elevation; it is negative since the objects are underground.

#	M Am^2	I deg	D deg	X m	Y m	Z m
42	0.561	65.53	-60.28	168.74	114.40	-0.89
43	0.652	52.00	192.22	101.44	101.75	-0.93
44	0.355	55.81	-112.72	171.41	124.46	-0.95
45	0.763	42.03	90.80	115.70	127.60	-0.95
46	0.159	-60.28	-49.49	169.00	138.50	-0.96
47	1.102	65.53	-60.28	169.53	115.44	-0.98
48	0.981	-4.00	-77.28	133.03	128.70	-1.06
49	0.419	8.19	80.95	165.10	121.46	-1.18
50	2.220	9.74	156.95	125.46	104.46	-1.23
51	0.819	50.86	-7.47	168.69	128.85	-1.23
52	0.938	66.52	124.64	125.00	139.50	-1.24
53	2.829	65.53	-60.28	167.66	114.23	-1.26
54	1.137	10.30	80.11	142.68	141.06	-1.32
55	2.011	30.17	71.30	150.17	108.85	-1.35
56	4.023	60.63	104.08	126.70	104.88	-1.47
57	1.212	22.87	104.86	115.57	131.64	-1.47
58	3.872	67.89	277.39	174.89	140.13	-1.50
59	2.134	36.53	136.10	103.88	106.89	-1.58
60	1.923	38.00	195.22	102.04	103.00	-1.61
61	2.688	41.75	176.90	133.80	127.00	-1.79
62	5.460	42.81	-226.04	128.03	143.14	-2.06
63	3.237	35.26	177.19	110.25	109.00	-2.14
64	3.522	39.10	141.41	121.39	134.28	-2.21
65	1.835	27.82	162.24	170.00	128.00	-2.26
66	4.190	40.88	188.22	130.46	128.74	-2.33
67	4.800	55.95	211.53	132.50	132.00	-2.34
68	692.266	86.18	208.44	123.85	116.10	-2.38
69	18.291	42.77	-112.29	125.84	135.22	-2.38
70	329.688	86.18	208.44	120.62	115.55	-2.50
71	3.862	31.03	227.81	157.50	113.79	-2.58
72	105.946	58.32	240.75	113.24	99.82	-2.70
73	287.239	76.42	108.35	140.32	102.40	-3.31
74	675.424	32.83	131.37	104.22	138.81	-3.44
75	217.770	76.42	108.35	151.66	126.03	-3.72
76	1136.250	86.18	208.44	110.41	118.78	-4.69
77	841.610	76.42	108.35	141.38	117.63	-4.87
78	821.314	32.83	131.37	105.97	133.99	-5.07
79	1290.000	86.18	208.44	118.61	116.86	-5.99
80	1012.067	32.83	131.37	105.85	127.16	-6.97
81	2762.421	76.42	108.35	138.24	105.60	-7.44
82	1847.663	76.42	108.35	145.75	123.11	-8.90

Figure 39: Further dipolar parameters. These were sorted by the estimates of depth (Z), and the deepest bodies are listed here. Parameter M is the magnetic moment of each body, while the ID angle describes the direction of total magnetization.

The depth weighting function for the
Geonics EM38 electromagnetic induction meter
operating it its magnetic susceptibility mode
with its magnetic dipoles vertical.

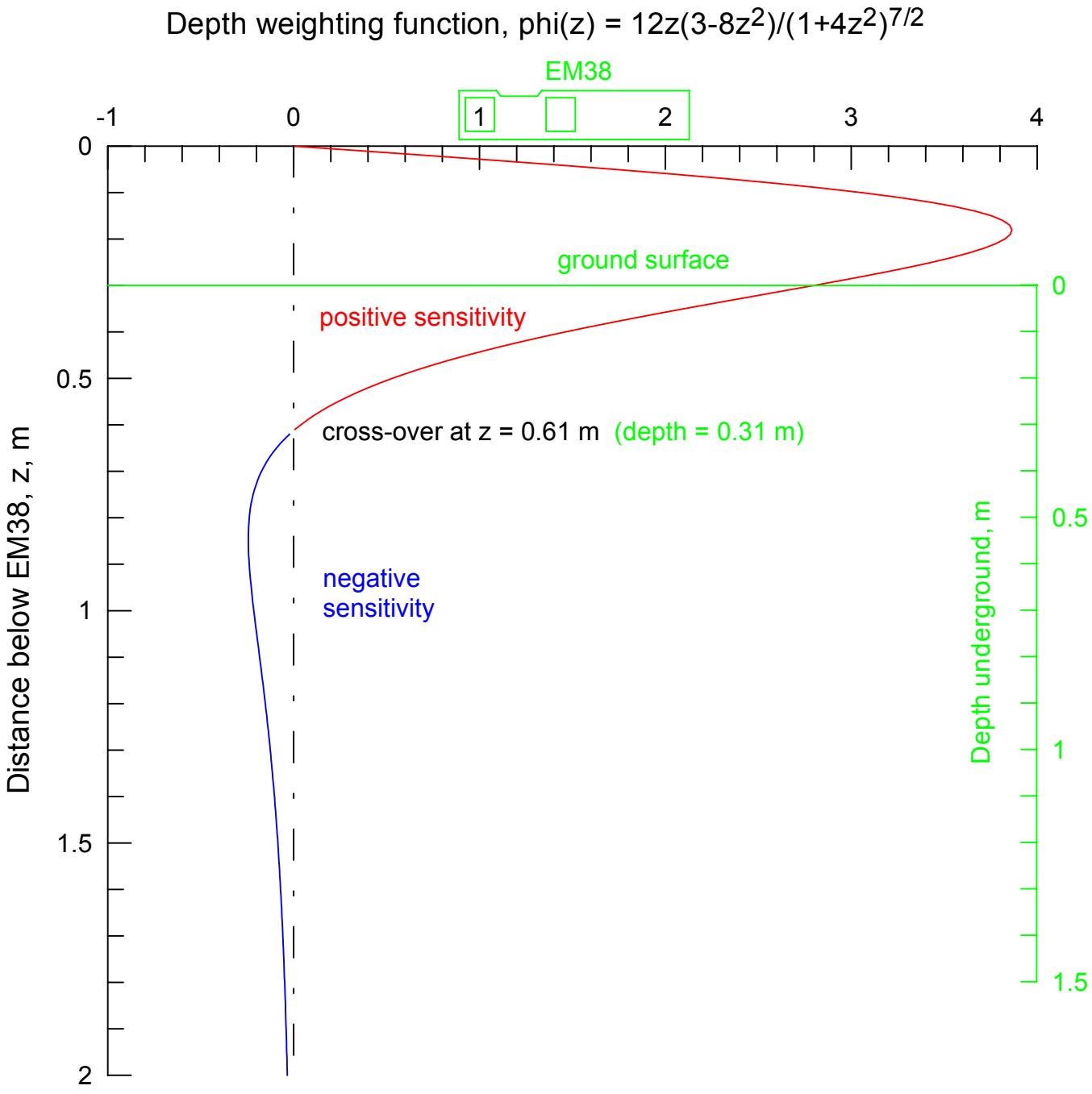

Figure 40: The depth sensitivity of the EM38 in its magnetic susceptibility mode. When it is raised to a height of 0.3 m (as it was for this survey), soil strata and features that are shallower than 0.3 m cause high or positive readings, while strata and features that are deeper can cause lower or negative readings of apparent susceptibility. The depth-weighting function was supplied by Duncan McNeill (Geonics). While most of the sensitivity of the EM38 is "wasted" by measuring the susceptibility of the air, the operational height of 0.3 m was needed because of the tall grass.

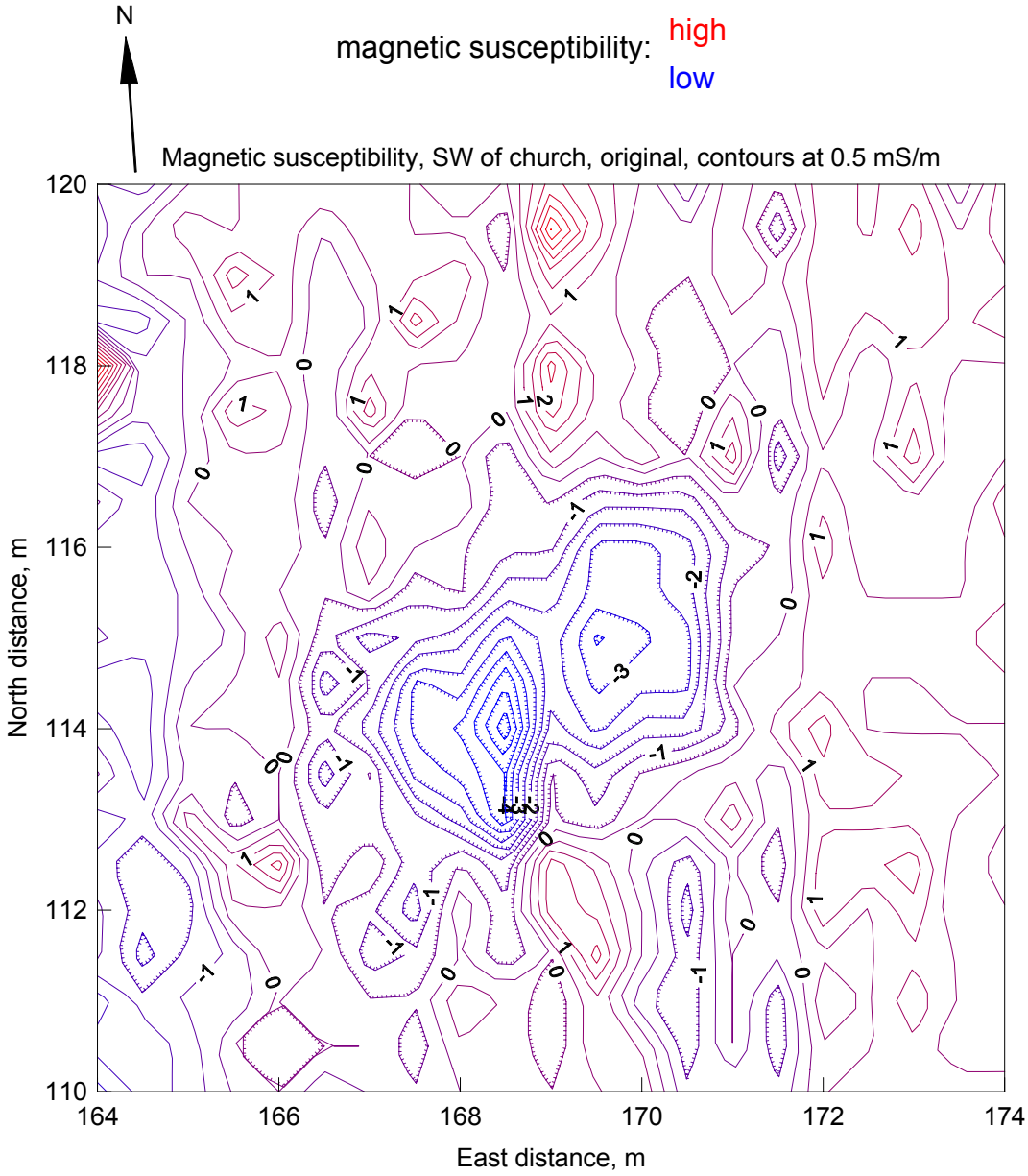

Figure 41: The original measurements of magnetic susceptibility. These were recorded in the area of the detailed survey southwest of the church. Traverses were made to the north or south, and the readings are seen to fluctuate from line to line in this map. These errors were later corrected in the final map that is plotted in Figure 23.

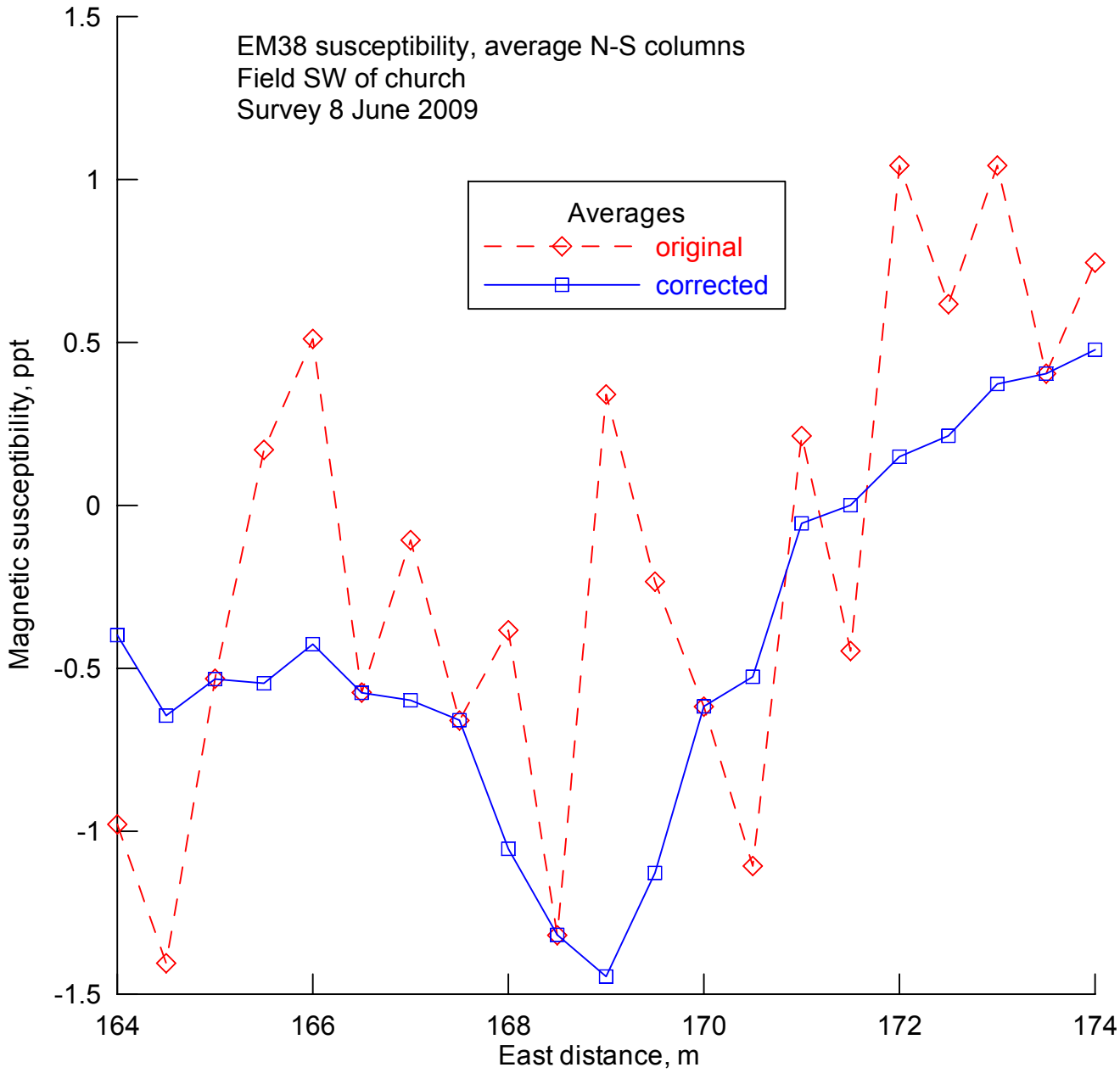

Figure 42: Irregularities between lines of EM38 readings. The average reading along each line of measurement is plotted here. The original readings were quite variable, due to an improper procedure that was applied in the field. When the average of each line was forced to a smooth curve, the final values were more consistent from line to line.

Figure 43: The resistivity survey. Bruce is carrying the resistivity meter with a strap around his neck. The two poles in front locate the moving electrodes for the pole-pole survey. The measurements were recorded with pencil in a notebook. Several graves are visible in the yard of the church. This photo was supplied by Marit Synnøve Vea.

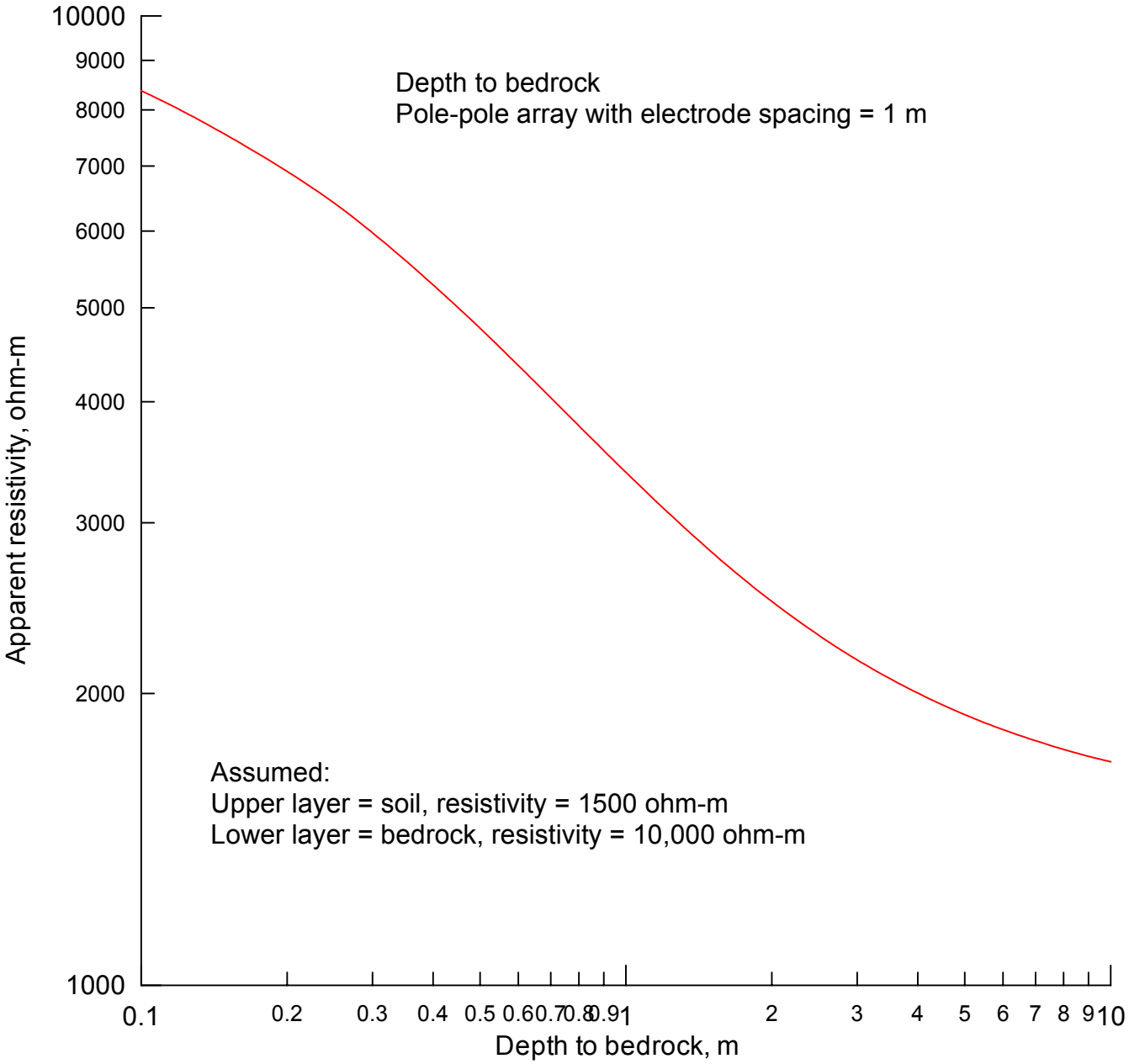

Figure 44: Analysis of the resistivity readings. This allows an estimate of the thickness of soil over bedrock. It was possible to estimate the resistivity of both the soil and the bedrock at this site. If these estimates are correct, then the resistivity readings can be converted to indications of the thickness of the soil with the aid of this curve.